

Nanoemulsion adjuvantation strategy of tumor-associated antigen therapy rephrases mucosal and immunotherapeutic signatures following intranasal vaccination

Chung-Hsiung Huang,¹ Chiung-Yi Huang,² Hui-Min Ho,² Ching-Hung Lee,² Pang-Ti Lai,^{2,3} Suh-Chin Wu,³ Shih-Jen Liu,^{2,4,5} Ming-Hsi Huang ^{2,4,5}

To cite: Huang C-H, Huang C-Y, Ho H-M, *et al.* Nanoemulsion adjuvantation strategy of tumor-associated antigen therapy rephrases mucosal and immunotherapeutic signatures following intranasal vaccination. *Journal for ImmunoTherapy of Cancer* 2020;**8**:e001022. doi:10.1136/jitc-2020-001022

► Additional material is published online only. To view please visit the journal online (<http://dx.doi.org/10.1136/jitc-2020-001022>).

Accepted 28 August 2020



© Author(s) (or their employer(s)) 2020. Re-use permitted under CC BY-NC. No commercial re-use. See rights and permissions. Published by BMJ.

¹Department of Food Science, National Taiwan Ocean University, Keelung, Taiwan

²National Institute of Infectious Diseases and Vaccinology, National Health Research Institutes, Miaoli, Taiwan

³Institute of Biotechnology, National Tsing Hua University, Hsinchu, Taiwan

⁴Graduate Institute of Biomedical Sciences, China Medical University, Taichung, Taiwan

⁵Graduate Institute of Medicine, Kaohsiung Medical University, Kaohsiung, Taiwan

Correspondence to

Dr Ming-Hsi Huang;
huangminghsi@nhri.org.tw

ABSTRACT

Background Emulsion adjuvants are a potent tool for effective vaccination; however, the size matters on mucosal signatures and the mechanism of action following intranasal vaccination remains unclear. Here, we launch a mechanistic study to address how mucosal membrane interacts with nanoemulsion of a well-defined size at cellular level and to elucidate the impact of size on tumor-associated antigen therapy.

Methods The squalene-based emulsified particles at the submicron/nanoscale could be elaborated by homogenization/extrusion. The mucosal signatures following intranasal delivery in mice were evaluated by combining whole-mouse genome microarray and immunohistochemical analysis. The immunological signatures were tested by assessing their ability to influence the transportation of a model antigen ovalbumin (OVA) across nasal mucosal membranes and drive cellular immunity *in vivo*. Finally, the cancer immunotherapeutic efficacy is monitored by assessing tumor-associated antigen models consisting of OVA protein and tumor cells expressing OVA epitope.

Results Uniform structures with ~200 nm in size induce the emergence of membranous epithelial cells and natural killer cells in nasal mucosal tissues, facilitate the delivery of protein antigen across the nasal mucosal membrane and drive broad-spectrum antigen-specific T-cell immunity in nasal mucosal tissues as well as in the spleen. Further, intranasal vaccination of the nanoemulsion could assist the antigen to generate potent antigen-specific CD8+ cytotoxic T-lymphocyte response. When combined with immunotherapeutic models, such an effective antigen-specific cytotoxic activity allowed the tumor-bearing mice to reach up to 50% survival 40 days after tumor inoculation; moreover, the optimal formulation significantly attenuated lung metastasis.

Conclusions In the absence of any immunostimulator, only 0.1% content of squalene-based nanoemulsion could rephrase the mucosal signatures following intranasal vaccination and induce broad-spectrum antigen-specific cellular immunity, thereby improving the efficacy of tumor-associated antigen therapy against *in situ* and metastatic tumors. These results provide critical mechanistic insights into the adjuvant activity of nanoemulsion and give

directions for the design and optimization of mucosal delivery for vaccine and immunotherapy.

BACKGROUND

Nasal spray or intranasal vaccination is considered a promising strategy for inducing mucosal protection against respiratory tract infections and systemic immunity with long-lasting memories¹; however, antigen applied to mucosal membranes generally induces minuscule immune responses owing to mucosal membrane barriers and immune tolerance.² Another obstacle for intranasal vaccination derives from evidence pointing to the toxin-based nasal adjuvants posing a risk of inoculum invasion into the central nervous system.^{1,2} Therefore, the aid of a safe mucosal adjuvant with high efficacy is necessary for antigen recognition by the mucosal immune system and generation of broad-spectrum immune responses.

Emulsion adjuvants are a potent tool for effective vaccination against infectious disease and cancer.^{3–8} Despite progress in this field, no intranasal vaccine or immunotherapy formulated with this type of adjuvants is currently registered for human use to protect against or treat disease. Potential safety concerns and low immunity generated in a manner suitable for patients remain major challenges. Over the years, it has become clear that size is critical for adjuvant activities, and small-sized particles are considered more bioactive than large ones.⁹ One of the major explanations for this phenomenon is that particles with a smaller size have a larger surface area, which is beneficial for antigen loading and particle–cell interactions.¹⁰ Another explanation is that particles at the nanoscale are most effective for antigen delivery across

mucosal surface barriers compared with larger sized ones.^{10,11} With respect to immunological effects, different size ranges of particles may result in different levels and qualities of immune responses. Although the relationship between particle size and the generated immune profile remains controversial, some studies have substantiated that particles with a size ranging from 20 to 200 nm are mainly internalized by immune cells via endocytosis, leading to the dominant cellular immune responses.¹¹ In contrast, particles in the size range of 0.5–5 μm are usually targeted to phagocytic cells *in vivo*, resulting in the major humoral immune responses.¹¹ Accordingly, the development of a particle-based mucosal adjuvant at the nanoscale is suggested as a potential strategy to deliver antigens across mucosal barriers and elicit concomitant cell-mediated immune responses.

We have previously optimized a ready-to-use emulsion adjuvant dubbed PELC, which is cored by squalene (an isoprenoid hydrocarbon with six unsaturated double bonds) and emulsified by Span85 (sorbitan trioleate) and a bioresorbable polymer poly(ethylene glycol)-*block*-poly(lactide-*co*-ε-caprolactone) (PEG-*b*-PLACL), suspending in phosphate-buffered saline (PBS).^{4–7} Following parenteral injection, our results suggest that unsaturated squalene oil was more powerful than saturated squalene oil to induce reactive oxidative species-mediated antigen uptake⁸; moreover, adjuvantation with the aid of PELC may be a prospective strategy to manipulate antigen-specific immune responses and to build on rational vaccine design and fabrication in prophylactic and therapeutic applications.^{5–7} However, intranasal

vaccination with PELC in the absence of immunomodulatory agents does not elicit forceful immune responses,^{4,5} and thus an appreciative condition for mucosal delivery should still be optimized.

Here we launch a mechanistic study that monodisperse nanoemulsion facilitates antigen transportation across the nasal mucosal membrane and thereby enhances vaccine efficacy, compared with free antigen vaccination (figure 1A). This investigation is brought to fruition by tailoring the PELC particles, originally polydisperse submicron structure, to monodisperse nanosized distribution by progressively passing through extruder membranes. We choice chicken ovalbumin (OVA) as model antigen to further understand the signatures of the monodisperse nanoemulsion interacting with mucosal membranes in mice and to elucidate their roles in vaccine immunogenicity following intranasal vaccination. In the beginning, we investigate whether monodisperse nanoemulsion can facilitate the transportation of antigen across the mucosal membrane to the site of immune induction, the nasal-associated lymphoid tissue (NALT),¹² compared with polydisperse ones. The immunological signatures of these formulations are then tested by assessing their ability to drive broad-spectrum mucosal and splenic cellular immunity via intranasal vaccination. Finally, the adjuvant efficacy is examined by assessing codelivery of OVA protein with monodisperse nanoemulsion to achieve a successful immunotherapy by delivering a stronger cytotoxic T lymphocyte (CTL) response to kill antigen-transfected cells, and the respective mode of adjuvant action is proposed.

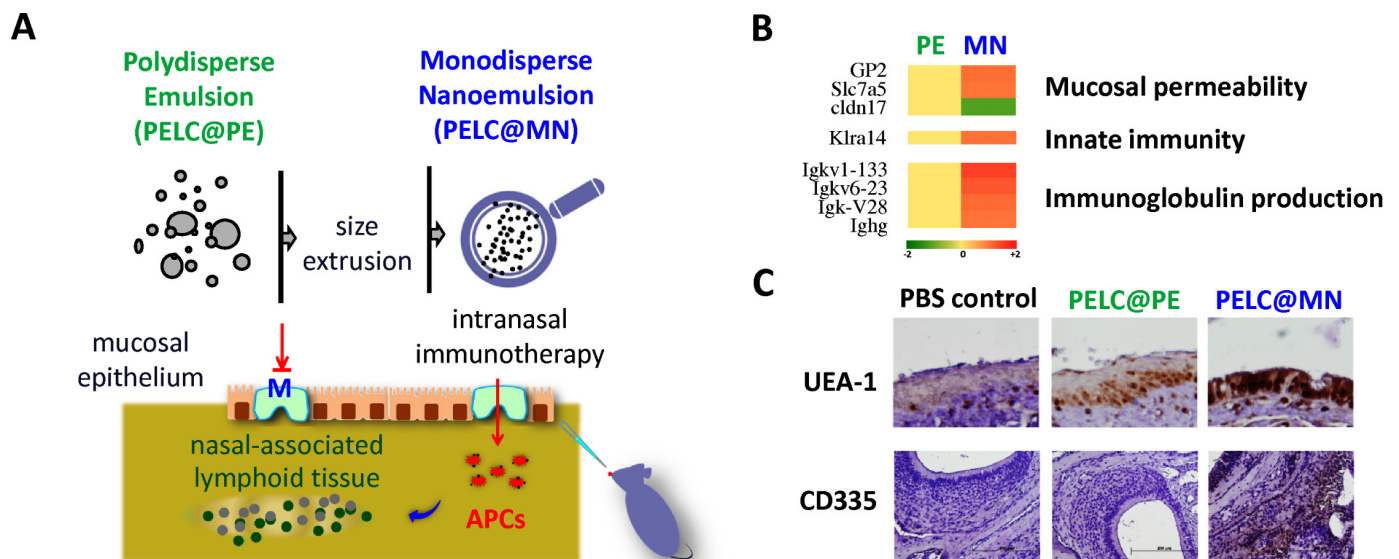


Figure 1 Tailoring emulsified particles to monodisperse nanosized distribution rephrases mucosal signatures following intranasal vaccination. (A) Schematic illustration of the monodisperse nanoemulsion enables the antigens to pass through the mucosal epithelium and facilitate the transportation of antigens into lymphoid tissues. (B) Microarray analysis of transcription profiles induced by emulsified particles 20 hours after administration. Genes with a fold change ≥ 1.5 and $p < 0.05$ compared with the PBS control. (C) Membranous (M) cell emergence and natural killer (NK) cell trafficking in nasal mucosa. Nasal mucosal tissues were harvested and phenotyped by immunohistochemical (IHC) staining. The brown signal around the blue nucleus indicates UEA-1+ and CD335+ cells, respectively (magnification, 400×). APCs, antigen-presenting cells. PBS, phosphate-buffered saline.

MATERIALS AND METHODS

Study design

We propose/demonstrate that tailoring emulsified particles to the monodisperse nanosized distribution can play a role in facilitating the transportation of antigen across mucosal membrane to the NALT and thereby enhances vaccine efficacy, compared with the original polydisperse ones. All experiments were conducted independently at least twice. The production of antigen-specific immunity and tumor challenge studies were designed to evaluate the size matter of the emulsion adjuvants on the immunogenicity as well as tumor-associated antigen therapy in a mouse model with OVA as antigen. Pooled data are presented for the draining lymph node (LN) cells and T-cell immunity experiments to obtain sufficient replicates for each condition. The number of animals in each group was based on the minimum number of mice for statistical analysis and replicate experiments. Prior to treatment, the animals were randomized to minimize variances between groups. All materials injected into animals were determined to be free of mycoplasma.

Chemicals, reagents, antibodies and cell lines

Reagents and media for cell culture were purchased from Thermo Fisher Scientific (NY, USA) and GE Healthcare (Utah, USA). Reagents and standards for ELISA were purchased from R&D Systems (MN, USA). Antibodies used for flow cytometric analysis were purchased from BioLegend (CA, USA). The EG7 cell line (American Type Culture Collection, CRL-2113) was maintained in complete RPMI 1640 medium supplemented with an aminoglycoside antibiotic Calbiochem G418 (0.4 mg/mL, Merck, Darmstadt, Germany). The B16-F10-OVA cell line was maintained in complete Dulbecco's modified Eagle's medium supplemented with 0.4 mg/mL of G418.

Emulsion preparation

For PELC@PE preparation, a mixture comprising 120 mg of diblock copolymer PEG-*b*-PLACL, 0.8 mL of PBS, 0.935 mL of squalene and 0.165 mL of Span85 was first emulsified by means of a homogenizer (Polytron PT 2500E, Kinematica, Swiss), as previously described.⁵⁻⁷ Then, 200 μ L of the stock emulsion was redispersed into 1800 μ L of PBS in a test tube, and allowed to mix the emulsified suspension using a rotator at a mild condition (5 rpm) for 1 hour. Next, 10 μ L aliquot of a specimen was added to 990 μ L of PBS, rendering a final diluted sample (referred to as PELC@PE). For PELC@MN preparation, PELC@PE suspension was passed through polycarbonate membranes (Whatman Nuclepore Track-Etched Membranes, GE Healthcare, Darmstadt, Germany) mounted in a mini-extruder fitted with two 1.0 mL gas-tight syringes. Typically, 11 passages were performed to achieve a monodisperse distribution and to avoid contamination with the sample (an odd number of passages) that might not have passed through the membrane. After progressively passing through 1.0, 0.4, 0.2, and 0.1 μ m membranes, the emulsified particles were obtained with monodisperse

distribution and at the nanoscale (referred to as PELC@MN). The particle size distribution was measured by a particle size analyzer (Nano ZS, Malvern, Brookhaven Instruments, NY, USA). The microscopic aspects were monitored using an optical microscope (Olympus DP70) and a transmission electron microscopy (H-7650, Hitachi, Japan).

Mice

BALB/c and C57BL/6 female mice at age of 5 weeks were obtained from the National Laboratory Animal Breeding and Research Centre (Taipei, Taiwan) and acclimatized for 1 week at the Laboratory Animal Centre of the National Health Research Institutes (Miaoli County, Taiwan) prior to use.

Nasal mucosal gene expression analysis

BALB/c mice (n=3 per group) were intranasally administered in both nostrils with 10 μ L per nostril of PBS, PELC@PE or PELC@MN. Nasal mucosa was harvested from mice at 20 hours after administration. Parts of the mucosal samples were used for total RNA extraction with TRI Reagent (Sigma-Aldrich) according to the manufacturer's instructions, and the other parts were prepared for immunohistochemical (IHC) staining. Prior to hybridization, the quality and integrity of the RNA samples were determined using an Agilent 2100 Bioanalyzer. Hybridization was performed using Mouse Gene 2.0 ST array (Affymetrix, CA, USA), and the microarrays were scanned by a Molecular Devices GenePix 4000B Scanner according to the manufacturer's guidelines. Gene expression values were analyzed by gene set enrichment analysis.

IHC staining of nasal mucosal tissues

IHC was performed on 4–5 μ m sections of each paraffin block. The sections were deparaffinized and rehydrated by sequentially immersing into xylene and ethanol as previously described.⁶ For antigen retrieval, the hydrated slides of nasal mucosal and tumor tissues were immersed in Trilogy at 90°C for 30 min, followed with 3% hydrogen peroxide (H₂O₂) for 15 min to block the endogenous peroxidase activity. After washing with PBS, the slides were further blocked with 2.5% normal horse serum for 1 hour. The primary antibodies, anti-CD3, anti-CD4, anti-CD8, anti-CD335 NKp46 (BioLegend) and anti-UEA-1 (MBL, IL, USA), were applied, and the sections were then incubated at room temperature for 1 hour. After washing with PBS, the sections were further incubated with the peroxidase polymer detection kit (Nichirei Bioscience, Tokyo, Japan) for 1 hour. Finally, the slides were visualized by DAB staining, followed by hematoxylin counterstaining. The IHC-positive signals were observed and analyzed at a 400-fold magnification using an Olympus DP70 microscope. The number of IHC-positive signals and area of positive signal were quantified using the ImageJ image processing and analysis program (Bethesda, MD, USA). Three measurements per tissue section and three to six

sections per group were analyzed at 200-fold and 400-fold magnification.

Detection of OVA transportation

BALB/c mice (n=3 per group) were intranasally administered with OVA alone, OVA plus PELC@PE or OVA plus PELC@MN. The mice were sacrificed at 0, 4 and 20 hours after administration. The harvested nasal mucosal tissues were washed with saline and then fixed for 24 hours with 10% neutral buffered formalin. Tissue blocks and slides were prepared as mentioned above, and the anti-OVA antibody (BioLegend) was used for staining of OVA in mucosal tissues.

Vaccination and immunoassays

For immunological evaluation, BALB/c mice were vaccinated via the intranasal route with OVA formulations (100 µg/dose, 20 µL) once a week for 3 weeks. One week after the final vaccination, the mice (n=3 per group) were sacrificed to collect nasal mucosal tissues and spleen samples for further experiments.

Blocks and slides of nasal mucosal tissue were prepared as mentioned above, and anti-CD3, anti-CD4 and anti-CD8 antibodies (BD Biosciences, CA, USA) were used for IHC staining of T cells in the mucosal tissues.

Splenocyte suspensions were collected from the mouse spleen as described previously.^{6,7} Splenocyte suspensions (5×10^6 cells/mL) were cultured in the presence of OVA (10 µg/mL). At 24 hours, cell pellets in each group were prepared for extraction of total RNA using TRI Reagent (Sigma) according to the supplier's instruction. The steady-state mRNA expression levels, T-bet and ROR γ t, were measured by reverse transcription PCR in a manner similar to our previous study.⁶ The results are shown as the density ratio of the interest gene to the reference standard (β -actin). At 72 hours, the supernatants were collected from triplicate cultures and tested for interferon gamma (IFN- γ) and interleukin 17 (IL-17) concentrations (DueSet ELISA Development Kit, R&D Systems) following the manufacturer's instructions.

Phenotype and functional activation of CTLs

The antigen-specific CTL response was determined by analyzing the frequency of SIINFEKL-MHC-I tetramer+ CD8+ T cells. C57BL/6 mice (n=4 per group) were intranasally vaccinated with different OVA formulations (100 µg per dose, 20 µL) once a week for 3 weeks. One week after the final vaccination, splenocytes (5×10^6 cells/mL) harvested from vaccinated mice were treated with SIINFEKL (1 µg/mL) for 24 hours and stained with H-2Kb-restricted SIINFEKL tetramer, fluorescein isothiocyanate (FITC)-conjugated anti-CD8 and phycoerythrin (PE)-conjugated anti-CD107a antibodies on ice bath for 30 min. Samples were then examined by flow cytometry (LSRII; BD Immunocytometry Systems, CA, USA), and CD8+ T cells were gated for dot plot analysis of CD107a (PE) versus tetramer (APC, allophycocyanin). The

mean fluorescence intensity (MFI) of CD107a in gated CD8+H-2Kb/SIINFEKL+ cells was also determined.

Tumor challenge study

For in situ tumor model, a total of 2×10^5 EG7 tumor cells per mouse were first inoculated subcutaneously into the flank of C57BL/6 mice (n=6 per group). On the appearance of palpable tumors, the mice were intranasally vaccinated once a week for 3 weeks with 100 µg of OVA, non-formulated or formulated with candidate adjuvants. Tumor sizes were measured in two vertical dimensions using a digimatic caliper twice per week. Tumor volumes were calculated following the formula: (length \times width \times width)/2. For ethical issues, the mice were euthanized when they experienced severe faintness or when the tumor volume exceeded 2000 mm³.

For the lung melanoma metastatic model, C57BL/6 mice (n=6 per group) were injected intravascularly with B16-F10-OVA cells (5×10^5 cells/mouse). One week later, the mice were intranasally vaccinated once a week for 3 weeks with 100 µg of OVA, non-adjuvanted or adjuvanted with designed emulsions. One week after the final vaccination, the mice were sacrificed, and the lung was isolated for pathological observation.

Statistics

The statistical difference between each treatment group was assessed by Dunnett's two-tailed t-test using GraphPad Prism V.5.02 (GraphPad Software). P<0.05 was defined as significant. The median survival in tumor challenge study was calculated using the Gehan-Breslow-Wilcoxon method.

RESULTS

Tailoring emulsified particles to monodisperse nanosized distribution rephrases mucosal signatures following intranasal delivery

PELC suspensions issued from homogenization initially formed emulsified particles at the submicron scale with polydisperse distribution (termed PELC@PE for the remainder of this article). Such liquid-liquid colloids were soft and deformable so that the size could be controlled by passage through an extruder membrane (online supplemental figure S1). After sequential extrusion through membranes, as expected, particles with monodisperse nanosized distribution (termed PELC@MN for the remainder of this article) were observed with an average diameter of about 200 nm, which is consistent with the scale of nanoemulsion.¹³ In vitro results from our preliminary investigations show that monodisperse nanoemulsion with a well-defined size can dramatically induce activation of murine bone marrow-derived dendritic cells, compared with polydisperse emulsion (online supplemental figure S2). Subsequently, we plan to explore the adjuvant potency of the prepared emulsions to evaluate their remarkable mucosal activity and immunotherapeutic efficacy.

First, the innate immunological signatures following intranasal delivery were evaluated based on the impact of the monodisperse nanoemulsion on gene expression changes in nasal mucosal tissues. To achieve this goal, mice intranasally received 20 μ L of PELC@PE or PELC@MN diluted in PBS, and large-scale gene expression profiling of local mucosal tissues was performed at 20 hours after administration by whole-mouse genome microarray analysis. Among total genes screened, both PELC@PE and PELC@MN emulsions regulated a common set of 66 genes with a fold change ≥ 1.5 and $p < 0.05$ compared with the PBS treatment group (online supplemental tables S1–S3). Interestingly, PELC@MN regulated a larger number of genes (230) compared with PELC@PE (197), which were associated with categories including cell/mucosal permeability, immune responses, fatty acid metabolism, neurotransduction, oxidation and reduction, xenobiotic excretion, and so on (online supplemental table S4). Several genes associated with mucosal permeability, glycoprotein 2 (GP2),¹⁴ Slc7a5,¹⁵ cldn17,¹⁶ innate immunity (Klra14)¹⁷ and immunoglobulin production (Igkv1-133, Igkv6-23, Igk-V28, Ighg)¹⁸ were significantly regulated by PELC@MN compared with PELC@PE (figure 1B).

Concerning the results of microarray analysis, PELC@MN significantly upregulated the expression of numerous genes associated with mucosal permeability. Among these genes, GP2 was exclusively expressed on membranous (M) cells, which are specialized mucosal epithelial cells found in the mucosa-associated lymphoid tissues of nasal and intestinal mucosa and able to transport antigens across epithelial membrane for further interaction with immune cells.¹⁴ To further study the impact of size on inducing the emergence of M cells, the harvested nasal tissues were also assessed for IHC staining, and the slides were stained with anti-UEA-1, a common biomarker for M cells.¹⁴ As shown in figure 1C, more UEA-1+ cells were detected in PELC@MN-treated mice than in PELC@PE-treated and PBS-treated mice.

On the other hand, PELC@MN also altered the gene expression of Klra14, which represents a lectin-like receptor subfamily A expressed on natural killer (NK) cells.¹⁷ Therefore, we further investigated the impact of PELC@MN on the recruitment of NK cells to the nasal mucosa by IHC staining of CD335, a cytotoxicity-activating receptor that may be highly specific to NK cells.¹⁹ As shown in figure 1C, more CD335+ cells were detected in PELC@MN-treated mice than in PELC@PE-treated and PBS-treated mice. The findings from microarray analysis and IHC staining suggest that the increased mucosal permeability induced by PELC@MN may be associated with the greater number of M cells. In addition, PELC@MN may be used as a powerful tool in mucosal delivery of vaccine antigens and in the activation of innate immunity by increasing the number of activated NK cells.

Monodisperse nanoemulsion facilitates delivery of protein antigen across nasal mucosal membrane and drives broad-spectrum antigen-specific immunity

We next planned to assess the augmentation of mucosal permeability by PELC@MN in relation to adaptive immunity. We attempted to address whether PELC@MN could facilitate protein antigen transportation across the nasal mucosal membrane into NALT. Mice received intranasally with 50 μ g of OVA in both nostrils with either antigen alone or formulated with PELC@PE or PELC@MN. The nasal mucosal tissues were harvested at 0, 4 and 20 hours after administration and IHC stained with OVA antibodies. No OVA-positive signal was recognized in the IHC images of OVA-treated mice and PELC@PE-formulated OVA-treated mice within 20 hours (figure 2A), indicating an absence of OVA transportation across the nasal membrane. Brown signals (ie, OVA positive) were clearly induced in the nasal mucosal tissues of mice treated with PELC@MN-formulated OVA at 4 hours and increased progressively at 20 hours, that is, OVA transportation was strongly influenced by the presence of the PELC@MN particles, suggesting that PELC@MN could protect against the removal of protein antigen from the nasal cavity for at least 20 hours and deliver antigen across the mucosal barrier and into NALTs.

Cellular immunity has the prospect to play an important role in mucosal protection; there is evidence that memory T-cell populations, which are inherent in mucosal tissues, can respond rapidly and directly to infiltrating pathogens.^{19, 20} Thus, we investigated the impact of the monodisperse nanoemulsion on populations of mucosal T cells following intranasal vaccination. As shown in figure 2B and online supplemental figure S3, OVA alone had no impact on the number of CD3+, CD4+ and CD8+ T cells in the nasal mucosal tissues compared with the PBS control group. Notably, vaccination with PELC@MN-adjuvanted OVA induced a dramatic increase in the numbers of T-cell subsets in the surface as well as the lamina propria of nasal mucosal tissues; however, the effect was rather diminished when the adjuvant was replaced with PELC@PE. We further confirmed the importance of the monodisperse nanoemulsion on the functional activation of splenic T cells, which were harvested from the vaccinated mice following incubation of cells in vitro with OVA antigen (figure 2C). Concerning the cytokine secretion, PELC@MN was the most potent inducer of IFN- γ , a predominant T helper type 1 (Th1) cytokine, whereas IFN- γ secretion induced by PELC@PE-adjuvanted OVA was measured at the same level as OVA alone. Similarly, PELC@MN-adjuvanted OVA enhanced notable IL-17 secretion (the major Th17 cytokine) compared with those in the non-adjuvanted and PELC@PE-adjuvanted groups. This finding indicated that OVA at the dose of 100 μ g did not elicit adaptive responses; in addition, the presence of PELC@PE did not alter the situation. Concordantly, the mRNA expression levels of T-bet (Th1 type) and ROR γ t (Th17 type) were also significantly elevated in the PELC@MN-adjuvanted OVA group. Based on the above results,

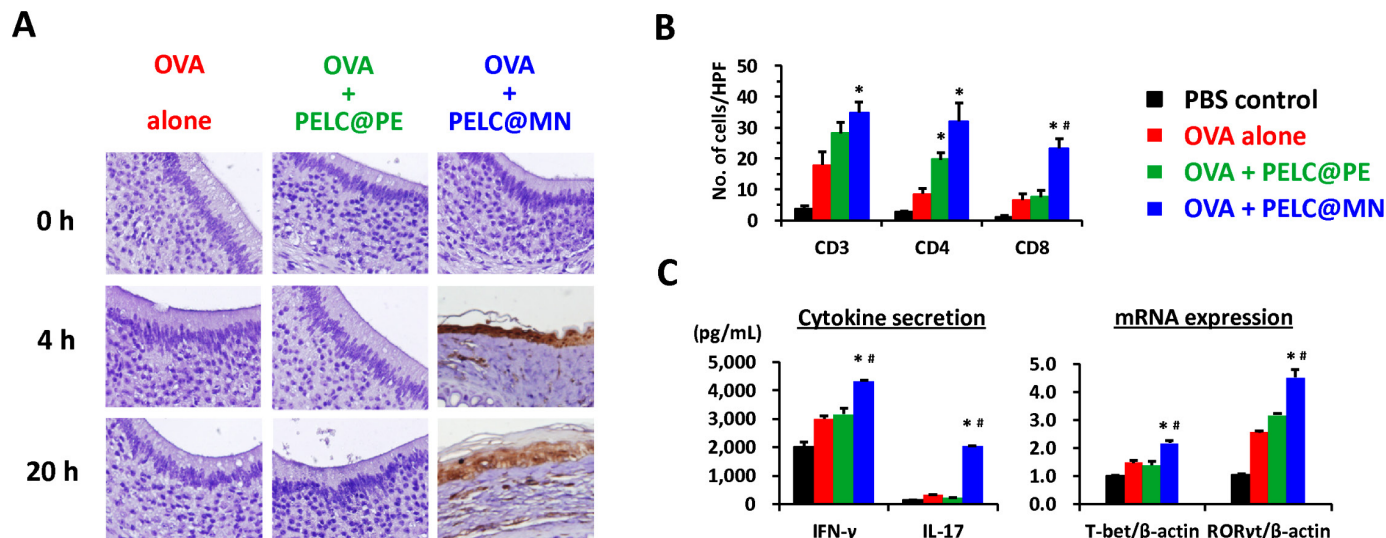


Figure 2 Monodisperse nanoemulsion facilitates the delivery of protein antigen across nasal mucosal membranes and drives broad-spectrum antigen-specific immunity in mice. (A) Transportation of OVA across nasal mucosal membranes. The nasal mucosal tissues were harvested from the treated mice and immunohistochemical (IHC) stained with OVA antibodies. The brown signals indicate OVA-positive signals (magnification, 400 \times). One week after the final administration, the mice (n=3) were sacrificed, and then nasal mucosal tissues and spleen were harvested for T-cell immunoassays. (B) T-cell subsets in nasal mucosal tissues. Observe microscopic fields using a power of 400 \times (see also online supplemental figure S3). (C) T-cell immunity in the spleen. The cell pellets were collected for mRNA expression of T-bet, ROR γ t and β -actin by reverse transcription PCR (RT-PCR), respectively. The supernatants were collected to measure IL-17 and IFN- γ secretion by ELISA. Data are expressed as the means \pm SEM. The results are representative of two to three independent experiments. *P<0.05 compared with OVA alone. #P<0.05 compared with the polydisperse emulsion group. HPF, high-power field; IFN- γ , interferon gamma; IL-17, interleukin 17; OVA, ovalbumin; PBS, phosphate-buffered saline.

emulsified particles with monodisperse distribution and at the nanoscale should be regarded as simple delivery systems for the delivery of antigen across the mucosal barrier and into NALTs and can play an active role in mediating Th1 and Th17 immune responses.

Monodisperse nanoemulsion assists antigen in generating potent antigen-specific CD8 $^{+}$ CTLs as well as antitumor ability when combined with tumor-associated antigen therapy

The phenotype and functional activation of CD8 $^{+}$ CTLs are critical characteristics in the clearance of virus-infected cells and in the defense against cancers.²¹ To test the potency of the monodisperse nanoemulsion to trigger the antigen-specific CTL response, we analyzed the frequency of SIINFEKL-MHC-I tetramer $^{+}$ CD8 $^{+}$ T cells. OVA-restimulated splenocytes were stained with a fluorescence-labeled anti-CD8 antibody and a fluorescence-conjugated SIINFEKL/MHC-I tetramer (where SIINFEKL is the H-2Kb-restricted OVA MHC class I epitope).²¹ As the benchmark, we also evaluated the elicitation of antigen-specific CTLs by analyzing the expression of CD107a on CD8 $^{+}$ H-2Kb/SIINFEKL $^{+}$ cells. In the literature regarding CD8 $^{+}$ T-cell degranulation, CD107a expression is closely associated with both cytokine secretion and cell-mediated lysis of target cells.²² As shown by flow cytometric analysis (figure 3A), the percentage of CD8 $^{+}$ H-2Kb/SIINFEKL $^{+}$ cells in splenocytes was approximately 1% in mice vaccinated with OVA alone and PELC@PE-adjuvanted OVA. Notably, the population of CD8 $^{+}$ H-2Kb/SIINFEKL $^{+}$ cells was significantly

increased to 5% in the vaccinated PELC@MN-adjuvanted OVA group, indicating that PELC@MN is able to induce the expansion of antigen-specific CD8 $^{+}$ CTLs via intranasal delivery. In addition, the MFI of the activation marker CD107a on gated CD8 $^{+}$ H-2Kb/SIINFEKL $^{+}$ cells was markedly increased from 70 to 551 in mice vaccinated with PELC@MN-adjuvanted OVA (figure 3B). However, the potency was slightly reduced when the adjuvant was replaced with PELC@PE. These results substantiated that PELC@MN emulsion as a mucosal adjuvant is capable of driving the expansion and activation of antigen-specific CTLs.

We conducted two murine models to evaluate whether the antigen-specific cytotoxicity in vivo reflected effective clearance of antigen-transfected cells. First, we applied an in situ tumor consisting of OVA protein/EG7 cells (OVA-transfected EL4 murine thymoma cells) as a tumor antigen/tumor cell model.⁶ All mice were first inoculated subcutaneously with EG7 tumor cells, and then they were vaccinated intranasally with OVA antigen, alone or adjuvanted with either PELC@PE or PELC@MN on days 7, 14 and 21. Figure 3C,D shows the monitored tumor volume and survival rate. The tumors grew progressively in the PBS control group (to mimic the tumor-bearing mice without receiving any treatment), and the mice started to die within 30 days. All mice that received non-adjuvanted OVA died before day 42, indicating that no protection for the mice received OVA alone. Vaccination of mice with OVA plus PELC@PE provided a better protective

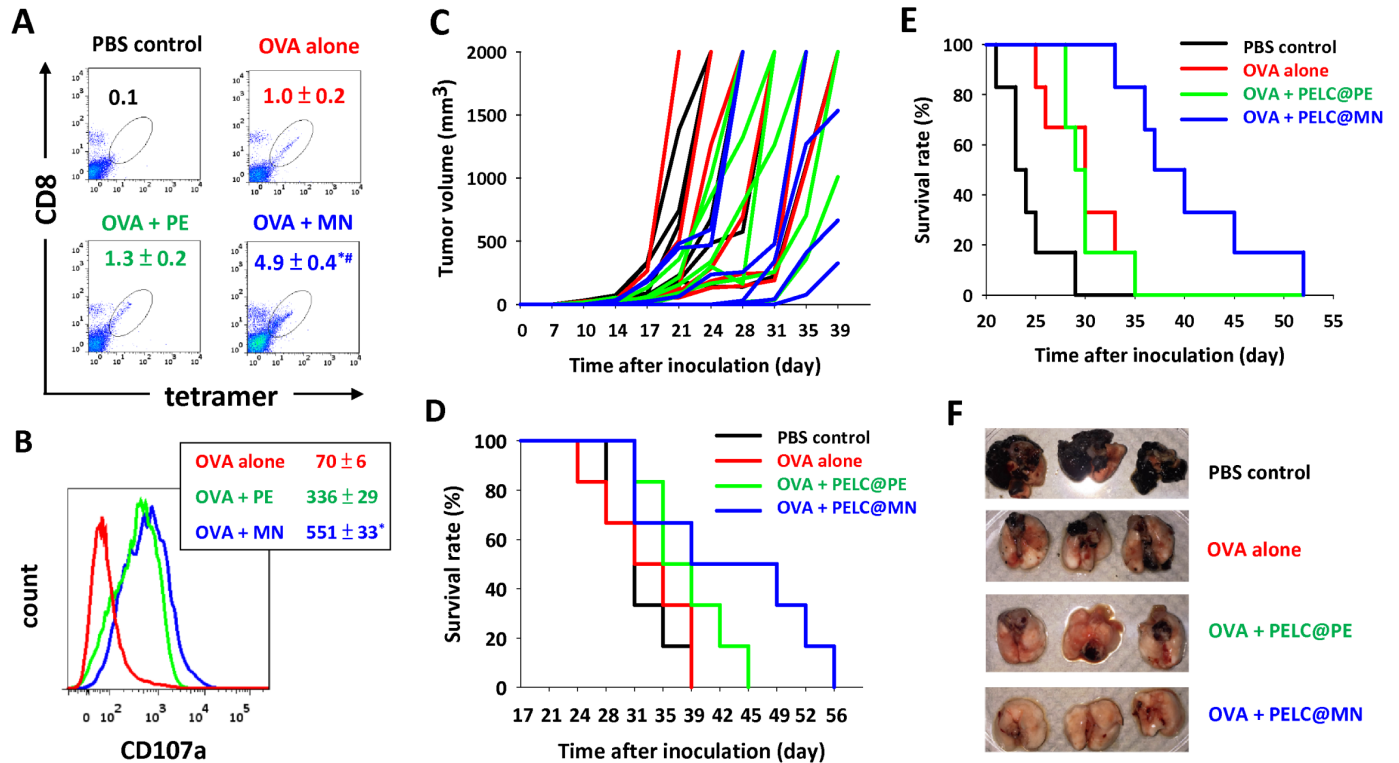


Figure 3 Intranasal delivery of monodisperse nanoemulsion could generate potent antigen-specific CD8⁺ cytotoxic T lymphocytes (CTLs) as well as clearance of antigen-transfected cells when combined with tumor-associated antigen therapy. Expansion and activation of antigen-specific CD8⁺ T cells. (A) The antigen-specific CTL response was determined by SIINFEKL-MHC-I tetramer staining and flow cytometry. (B) The mean fluorescence intensity (MFI) of CD107a on CD8⁺ T cells. Data are expressed as the mean \pm SEM from individual murine splenic sample. Intranasal delivery of PELC@MN-adjuvanted OVA inhibits tumor in situ. The mice (n=6) were first subcutaneously inoculated in the flank with EG7 tumor cells (1×10^5 cells per mouse). Seven days after tumor cell inoculation, the mice in each group were intranasally vaccinated with 100 μ g per dose OVA protein without or with either PELC@PE or PELC@MN on days 7, 14 and 21. (C) Tumor volume and (D) survival rate. Intranasal delivery of PELC@MN-adjuvanted OVA inhibits lung metastasis. The mice (n=6) were intravascularly inoculated with B16-F10-OVA cells (5×10^5 cells per mouse). One week later, the mice were intranasally vaccinated once a week for 3 weeks with OVA (100 μ g per dose), alone or adjuvanted with either PELC@PE or PELC@MN. (E) The survival rate was monitored two to three times per week. (F) Lung tissues at day 28 after inoculation of tumor cells. *P<0.05 compared with OVA alone. #P<0.05 compared with the PELC@PE group. OVA, ovalbumin; PBS, phosphate-buffered saline.

effect than those treated with OVA alone; however, it still not eradicates the inoculated EG7 cells. It is worthy to note that PELC@MN was better able than PELC@PE to broaden the immunotherapeutic efficacy of tumor-associated antigen (OVA) and to prolong the median survival of tumor cell (EG7)-bearing mice from 37 to 44 days. Last but not least, only the treatment with PELC@MN-adjuvanted OVA allowed the mice to reach up to 50% survival 40 days after tumor inoculation.

We next targeted immunotherapy for the treatment of cancer cell migration. In this approach, B16-F10-OVA (a stable transfectant murine OVA-expressing B16-F10 melanoma) was inhibited by vaccination with OVA in a metastatic cancer model.⁷ C57BL/6 mice that were intravascularly inoculated with B16-F10-OVA and then intranasally vaccinated three times at a 1-week interval with PELC@MN-adjuvanted OVA showed inhibited growth in tumor-bearing mice, compared with PELC@PE-adjuvanted OVA or OVA alone (figure 3E). Within 28 days, lethality started in the group of mice that did not get any treatment (PBS control). Although vaccination

with OVA alone or PELC@PE-adjuvanted OVA alleviated lung metastasis, all the mice in these two groups died before day 35. Notably, a remarkably small tumor volume and impressively high survival rate were observed in the group of mice who were vaccinated with PELC@MN-adjuvanted OVA (figure 3F), indicating that the aid of PELC@MN provided better protective capacity. These results demonstrate that intranasal vaccination of PELC@MN-adjuvanted OVA induced OVA-specific CTLs, which potentially killed OVA epitope-expressing cancer cells, suggesting that PELC@MN is a promising adjuvant for the development of an antitumor immunotherapeutic vaccine.

DISCUSSION

Based on the mechanisms of action, mucosal adjuvants could be classified into three categories, including immunostimulators, particulate adjuvants, and their combinations.¹⁻⁵ Immunostimulators, such as toll-like receptor agonists and bacterial toxins, have been assessed as

mucosal adjuvants for a long time^{3 23}; however, those made by the aforementioned compounds may sometimes be bombarded with medical risks for massive vaccination.³ Another concern is that mucosal epithelium is sometimes a barrier for targeting immune cells.³ To this, several delivery systems have been designed to transport antigens across mucosal barrier with diminutive obstruction and degradation by the mucociliary clearance system, mucin, and digestive enzyme.^{23 24} In recent decades, the development of particulate adjuvants at nanoscale, such as nanoemulsions, liposomes, micelles, and metal particulates, has attracted large amounts of attention due to their properties of small size, large surface area, and improved solubility and interactions with the biological environment.^{25 26}

The intake of fats or fatty acids may regulate or stimulate immune responses, such as lymphocyte proliferation, cytokine production, and phagocytosis.²⁷ Such regulation of immune responses may result from several factors, but the change in the cell membrane due to the incorporation of lipid is considered the major point.²⁸ Nevertheless, the intake of large oil globules may lead to non-specific immune reactions, such as delayed-type hypersensitivity, activation of NK cells and phagocytes, among others.²⁹ Thus, some studies suggest that PEGylation may be a generic strategy for the lipid squalene, enabling the efficient formation of nanoparticles in buffer solution by self-assembly.³⁰ Another strategy is to formulate the selected fats or fatty acids in the form of emulsions into vaccines to increase their immunogenicity and efficacy. Essentially, the good dispersion of oil drops in a vaccine formulation is crucial for the stability of the formulation, vaccine administration, evoking immune responses and attenuating local reactions.³¹ The oil-in-water emulsion adjuvant MF59 contains metabolizable squalene as the oily core, a lipophilic emulsifier Span85 and a hydrophilic Tween80 (polyoxyethylene sorbitan monooleate) suspended in buffer solution. MF59 has previously been demonstrated to be an effective adjuvant for parenteral injection but was not an effective adjuvant for intranasal vaccination with herpes simplex virus type 2 recombinant glycoprotein D2.²³ Although the adjuvant mechanism of MF59 following intranasal vaccination is not clear, the authors suggested physically associating the antigen with the adjuvant is necessary.²³ It has been reported that intranasal vaccination of vaccine candidates with a nanoemulsion containing cationic compound cetylpyridinium chloride induces strong and protective immune responses in rodents and ferrets towards the invaded pathogens.^{32 33} The potential mechanisms of action include sustained antigen adhesion to the mucosal membrane, induction of nasal epithelial cell apoptosis and heterogeneous cytokine production, transcellular antigen uptake in nasal epithelial cells and dendritic cells activation/trafficking to NALT.³²⁻³⁴ In the present study, we also substantiated that monodisperse squalene-cored emulsion at the nanoscale, that is, PELC@MN, sustained antigen retention at mucosal tissues for at least 20 hours

and transported antigen across the mucosal barrier (figure 2A).

In our previous studies, we demonstrated that the addition of immunostimulators, for example, recombinant flagellin,⁴ and synthetic peptide analog LD-indolicidin,⁵ into the PELC emulsion is necessary for successful intranasal vaccination against influenza virus. Herein, intranasal vaccination with PELC@MN could elicit potent cell-mediated immunity, especially Th1 and Th17 immune responses, without using any immunostimulator or cationic surfactant. Most importantly, PELC@MN could even increase the number of NK cells at the NALT, activate CD8+ CTLs, and attenuate lung metastasis, providing the complementary information of the potential of monodisperse nanoemulsions for cancer immunotherapy. Similar to cationic emulsions, PELC@MN increased heterogeneous cytokine mRNA expression at mucosal tissues. The effects of PELC@MN on delivering antigen across mucosal membrane and eliciting immune responses are closely associated with the elevated permeability of the mucosal membrane. Based on the results of microarray analysis, the induction of epithelial cell death is considered a potential mechanism for increasing mucosal permeability and heterogeneous cytokine production. Merging the results of the microarray analysis and IHC staining, the elevated permeability may be due to the increase in transcellular and/or paracellular transport. In the transcellular pathway, the increase of nasal mucosal permeability is supported by the expression of M cells (figure 1B). On the other hand, the paracellular pathway involves the transport of protein antigen through the tight junctions between the epithelial cells, which is highly restricted for smaller particles (online supplemental figure S1). These findings were in agreement with literature data, which demonstrated that nanoparticles could surmount nasal epithelial barrier, so as that antigen presenting properties can be initiated.^{11 25} Regarding this, further studies are warranted to verify the speculated mechanism of action of PELC@MN at the molecular level.

It has been demonstrated that the cytotoxic effects of NK cells and CD8+ CTLs contribute to protection against tumor metastasis.³⁵ Previous studies in IL-17-deficient mice have reported that the augmented growth and metastasis of tumor potentially resulted from the diminished number of NK cells and tumor-specific IFN- γ + T lymphocytes in tumor microenvironment as well as draining lymph nodes.³⁶ Accordingly, the adjuvant activity of PELC@MN against lung metastasis may be mediated by its effects on elevating the number of NK cells and inducing the activation of Th1, Th17 and CTL cells. With this potential in mind, further investigations are underway to launch the translation of the nanoemulsion adjuvantation strategy to human clinical trials for elucidating the feasibility of nanoemulsion as mucosal adjuvants and/or spraying delivery for the prevention and treatment of infectious diseases and cancers. Research is needed to verify whether squalene nanoemulsion has

similar effects in a human tumor xenograft model based on HLA transgenic mouse. With the aim of extending our results to enhance the efficacy of immunotherapy candidates in clinical applications, the research setting is rationally designed to investigate immunotherapeutic treatments comprising tumor-associated antigen therapy and immune checkpoint blockade therapy effectively reinforce each other via codelivery of tumor-associated antigens/immune checkpoint inhibitors with an optimal formulation towards enrichment of the immune micro-environments at local vaccination tissues, ipsilateral draining lymph nodes and tumor bed, thereby synergistically integrating the efficacy of individual cancer therapy. Such applications require nanoemulsion production at pilot scale in a consistent and reproducible manner which will be accomplished by homogenization with a high-shear microfluidized process.

CONCLUSIONS

In this study, we provided the comprehensive information demonstrating that tailoring emulsified particles to monodisperse nanosized distribution (assigned as PELC@MN) could rephrase mucosal and immunotherapeutic signatures following intranasal vaccination. Intranasal vaccination with tumor antigen adjuvanted with a squalene-cored PELC@MN significantly attenuated tumor growth and lung metastasis, probably due to the activation of innate immunity and cell-mediated immune responses. This hypothesis can be supported by several lines of evidence. First, intranasal vaccination with PELC@MN upregulated mucosal permeability, providing critical insights into the main action modes of PELC@MN as mucosal adjuvant. Second, the numbers of M cells and NK cells at mucosal sites were increased in mice after intranasally vaccinated with PELC@MN-adjuvanted OVA. Third, intranasal vaccination with PELC@MN-adjuvanted OVA markedly induced the activation of CD8⁺ cytotoxic lymphocytes as well as Th1 and Th17 cells, and thereby improved the efficacy of cancer immunotherapy against in situ and metastatic tumors. These results provide critical mechanistic insights into the adjuvant activity of monodisperse nanoemulsion and give directions for the design and optimization of mucosal delivery for vaccine and immunotherapy.

Twitter Ming-Hsi Huang @huangminghsi0

Acknowledgements PTL carried out his master's thesis research under the auspices of the Graduate Program of Biotechnology in Medicine, National Tsing Hua University and National Health Research Institutes. The authors are grateful to MOST for awarding a postdoctoral research scholarship to CHL (108-2811-B-400-519).

Contributors CHH performed the experiments, analyzed the data and wrote the paper. CYH, HMH, CHL, and PTL performed the experiments. SCW and SJL conceived the experiments. MHH managed the whole project, conceived the experiments and wrote the paper. All authors contributed to manuscript preparation.

Funding This work was supported by grant 109A1-IVPP19-014 from the National Health Research Institutes of Taiwan and grant 106-2314-B-400-016-MY3 from the Ministry of Science and Technology (MOST) of Taiwan.

Competing interests None declared.

Patient consent for publication Not required.

Ethics approval All animal studies were conducted in accordance with the established institutional guidelines and the approval protocols from the IACUC review board of NHRI (NHRI-IACUC-105125-A and NHRI-IACUC-105139-A).

Provenance and peer review Not commissioned; externally peer reviewed.

Data availability statement All data relevant to the study are included in the article or uploaded as supplementary information.

Open access This is an open access article distributed in accordance with the Creative Commons Attribution Non Commercial (CC BY-NC 4.0) license, which permits others to distribute, remix, adapt, build upon this work non-commercially, and license their derivative works on different terms, provided the original work is properly cited, appropriate credit is given, any changes made indicated, and the use is non-commercial. See <http://creativecommons.org/licenses/by-nc/4.0/>.

ORCID iD

Ming-Hsi Huang <http://orcid.org/0000-0002-9670-3821>

REFERENCES

- Ogra PL, Faden H, Welliver RC. Vaccination strategies for mucosal immune responses. *Clin Microbiol Rev* 2001;14:430–45.
- Buchon N, Broderick NA, Lemaître B. Gut homeostasis in a microbial world: insights from *Drosophila melanogaster*. *Nat Rev Microbiol* 2013;11:615–26.
- Wilson-Welder JH, Torres MP, Kipper MJ, et al. Vaccine adjuvants: current challenges and future approaches. *J Pharm Sci* 2009;98:1278–316.
- Lai C-H, Tang N, Jan J-T, et al. Use of recombinant flagellin in oil-in-water emulsions enhances hemagglutinin-specific mucosal IgA production and IL-17 secreting T cells against H5N1 avian influenza virus infection. *Vaccine* 2015;33:4321–9.
- Huang M-H, Dai S-H, Chong P. Mucosal delivery of a combination adjuvant comprising emulsified fine particles and LD-indolicidin enhances serological immunity to inactivated influenza virus. *Microbes Infect* 2016;18:706–9.
- Huang C-H, Huang C-Y, Cheng C-P, et al. Degradable emulsion as vaccine adjuvant reshapes antigen-specific immunity and thereby ameliorates vaccine efficacy. *Sci Rep* 2016;6:36732.
- Lin S-I, Huang M-H, Chang Y-W, et al. Chimeric peptide containing both B and T cells epitope of tumor-associated antigen L6 enhances anti-tumor effects in HLA-A2 transgenic mice. *Cancer Lett* 2016;377:126–33.
- Huang C-H, Huang C-Y, Huang M-H. Unsaturated squalene content in emulsion vaccine adjuvants plays a crucial role in ROS-mediated antigen uptake and cellular immunity. *Mol Pharm* 2018;15:420–9.
- Mumper RJ, Cui Z, Oyewumi MO. Nanotemplate engineering of cell specific nanoparticles. *J Dispers Sci Technol* 2003;24:569–88.
- Wendorf J, Singh M, Chesko J, et al. A practical approach to the use of nanoparticles for vaccine delivery. *J Pharm Sci* 2006;95:2738–50.
- Xiang SD, Scholzen A, Minigo G, et al. Pathogen recognition and development of particulate vaccines: does size matter? *Methods* 2006;40:1–9.
- Wu HY, Nguyen HH, Russell MW. Nasal lymphoid tissue (NALT) as a mucosal immune inductive site. *Scand J Immunol* 1997;46:506–13.
- Tadros T, Izquierdo P, Esquena J, et al. Formation and stability of nano-emulsions. *Adv Colloid Interface Sci* 2004;108-109:303–18.
- Ohno H, Hase K. Glycoprotein 2 (GP2): grabbing the FimH bacteria into M cells for mucosal immunity. *Gut Microbes* 2010;1:407–10.
- Poncet N, Halley PA, Lipina C, et al. Wnt regulates amino acid transporter SLC7A5 and so constrains the integrated stress response in mouse embryos. *EMBO Rep* 2020;21:e48469.
- Günzel D, Yu ASL. Claudins and the modulation of tight junction permeability. *Physiol Rev* 2013;93:525–69.
- Lee SH, Girard S, Macina D, et al. Susceptibility to mouse cytomegalovirus is associated with deletion of an activating natural killer cell receptor of the C-type lectin superfamily. *Nat Genet* 2001;28:42–5.
- Lefranc MP. Nomenclature of the human immunoglobulin kappa (IGK) genes. *Exp Clin Immunogenet* 2001;18:161–74.
- Freud AG, Zhao S, Wei S, et al. Expression of the activating receptor, NKp46 (CD335), in human natural killer and T-cell neoplasia. *Am J Clin Pathol* 2013;140:853–66.



- 20 Li AV, Moon JJ, Abraham W, *et al.* Generation of effector memory T cell-based mucosal and systemic immunity with pulmonary nanoparticle vaccination. *Sci Transl Med* 2013;5:204ra130.
- 21 Black M, Trent A, Kostenko Y, *et al.* Self-Assembled peptide amphiphile micelles containing a cytotoxic T-cell epitope promote a protective immune response in vivo. *Adv Mater* 2012;24:3845–9.
- 22 Alter G, Malenfant JM, Altfeld M. CD107a as a functional marker for the identification of natural killer cell activity. *J Immunol Methods* 2004;294:15–22.
- 23 Ugozzoli M, O'Hagan DT, Ott GS. Intranasal immunization of mice with herpes simplex virus type 2 recombinant GD2: the effect of adjuvants on mucosal and serum antibody responses. *Immunology* 1998;93:563–71.
- 24 Kirch J, Guenther M, Doshi N, *et al.* Mucociliary clearance of micro- and nanoparticles is independent of size, shape and charge--an ex vivo and in silico approach. *J Control Release* 2012;159:128–34.
- 25 Kamaly N, Xiao Z, Valencia PM, *et al.* Targeted polymeric therapeutic nanoparticles: design, development and clinical translation. *Chem Soc Rev* 2012;41:2971–3010.
- 26 Xiao Z, Su Z, Han S, *et al.* Dual pH-sensitive nanodrug blocks PD-1 immune checkpoint and uses T cells to deliver NF- κ B inhibitor for antitumor immunotherapy. *Sci Adv* 2020;6:eay7785.
- 27 de Pablo MA, Alvarez de Cienfuegos G. Modulatory effects of dietary lipids on immune system functions. *Immunol Cell Biol* 2000;78:31–9.
- 28 Clamp AG, Ladha S, Clark DC, *et al.* The influence of dietary lipids on the composition and membrane fluidity of rat hepatocyte plasma membrane. *Lipids* 1997;32:179–84.
- 29 Ahn YK, Kim JH. Effects of squalene on the immune responses in mice(II): Cellular and non-specific immune response and antitumor activity of squalene. *Arch Pharm Res* 1992;15:20–9.
- 30 Gaudin A, Song E, King AR, *et al.* PEGylated squalenoyl-gemcitabine nanoparticles for the treatment of glioblastoma. *Biomaterials* 2016;105:136–44.
- 31 Huang C-Y, Huang C-H, Liu S-J, *et al.* Polysorbosome: a colloidal vesicle contoured by polymeric bioresorbable amphiphiles as an immunogenic depot for vaccine delivery. *ACS Appl Mater Interfaces* 2018;10:12553–61.
- 32 Bielinska AU, Janczak KW, Landers JJ, *et al.* Mucosal immunization with a novel nanoemulsion-based recombinant anthrax protective antigen vaccine protects against Bacillus anthracis spore challenge. *Infect Immun* 2007;75:4020–9.
- 33 Hamouda T, Sutcliffe JA, Ciotti S, *et al.* Intranasal immunization of ferrets with commercial trivalent influenza vaccines formulated in a nanoemulsion-based adjuvant. *Clin Vaccine Immunol* 2011;18:1167–75.
- 34 Passmore C, Makidon PE, O'Konek JJ, *et al.* Intranasal immunization with W 80 5EC adjuvanted recombinant RSV rF-ptn enhances clearance of respiratory syncytial virus in a mouse model. *Hum Vaccin Immunother* 2014;10:615–22.
- 35 Guillerey C, Huntington ND, Smyth MJ. Targeting natural killer cells in cancer immunotherapy. *Nat Immunol* 2016;17:1025–36.
- 36 Kryczek I, Wei S, Szeliga W, *et al.* Endogenous IL-17 contributes to reduced tumor growth and metastasis. *Blood* 2009;114:357–9.

Supplementary Material

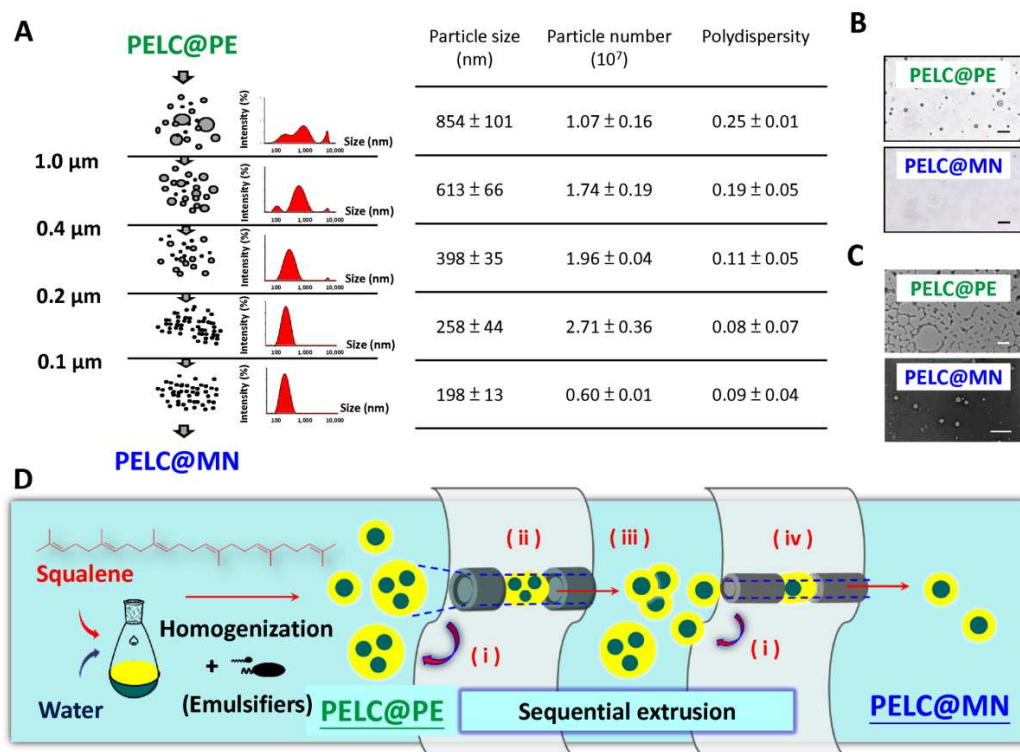
for

Nanoemulsion adjuvantation strategy of tumor associated antigen therapy rephrases mucosal and immunotherapeutic signatures following intranasal vaccination

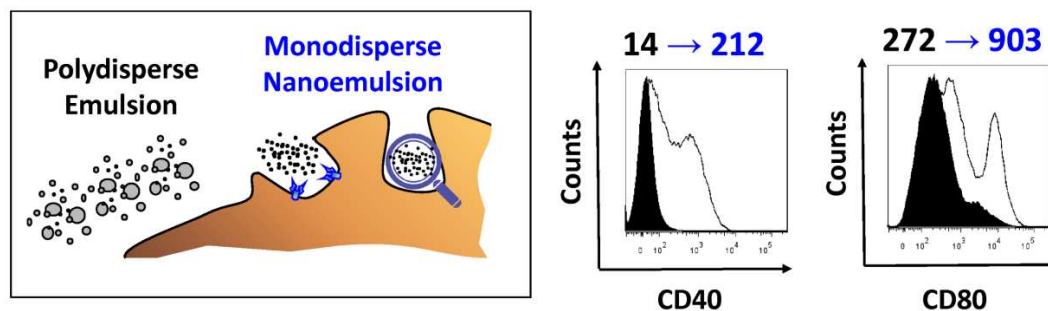
Chung-Hsiung Huang, Chiung-Yi Huang, Hui-Min Ho, Ching-Hung Lee, Pang-Ti Lai,
Suh-Chin Wu, Shih-Jen Liu, Ming-Hsi Huang

Correspondence to Dr Ming-Hsi Huang; huangminghsi@nhri.org.tw

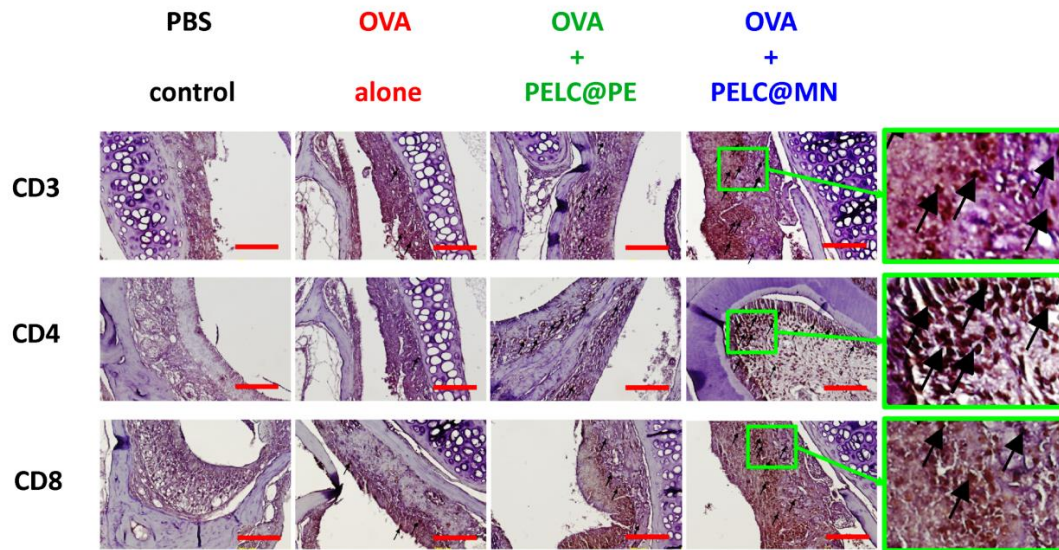
- Figure S1.** Nanoemulsion elaboration.
- Figure S2.** Activation of murine bone marrow-derived dendritic cells in vitro.
- Figure S3.** IHC staining of T-cell subsets in nasal mucosal tissues.
- Table S1.** Complete list of microarray selected hits having a p-value ≤ 0.05 and a fold change $\geq |1.5|$, PELC@PE vs PBS.
- Table S2.** Complete list of microarray selected hits having a p-value ≤ 0.05 and a fold change $\geq |1.5|$, PELC@MN vs PBS.
- Table S3.** Complete list of microarray selected hits having a p-value ≤ 0.05 and a fold change $\geq |1.5|$, PELC@MN vs PELC@PE.
- Table S4.** Core response gene list.



Supplementary Figure S1. Nanoemulsion elaboration. (A) DLS-measured particle size distribution of the emulsified particles following homogenization and sequential extrusion. Data are expressed as the means \pm standard deviation of three samples. (B) OM and (C) TEM images of PELC@PE and PELC@MN. Scale bars, 1 μm . (D) Schematic illustration of the proposed structure of the emulsified particles issued from homogenization and sequential extrusion (i) refraction; (ii) transformation; (iii) fracture; (iv) deformation. The particle size will still tend toward polydisperse distribution after the initial pass through a 1.0- μm membrane. The diameters of the emulsified particles are lower than the pore size of the membrane filters through 1.0 μm and 0.4 μm , probably due to the mechanisms comprising transformation and fracture which predominate the aspects of the particles; on the other hand, when the samples were extruded through filters with 0.2- μm and 0.1- μm membrane pores, the measured diameters were slightly higher than the pore size of the filter through which they were extruded. This feature may be attributed to the deformation nature of the particles. The recorded optical microscope (OM) images displayed PELC@PE was of spherical shape. Frustratingly, PELC@MN was invisible under OM mainly due to the light diffraction limit. The transmission electron microscopy (TEM) results showed that PELC@MN maintains spherical shape; it failed to capture the TEM images for PELC@PE because submicron squalene/water samples possess a rather low colloidal stability and will be fractured during fixation and dehydration.



Supplementary Figure S2. Activation of murine bone marrow-derived dendritic cells in vitro. Bone marrow-derived dendritic cells (BMDCs) were harvested from BALB/c mice, seeded at a density of 1×10^6 cells, and co-incubated with emulsified particles original polydisperse (PELC@PE, black area) or tailored monodisperse nanoemulsion (PELC@MN, white area) for 18 h. The expression levels of the costimulatory molecules CD40 and CD80 were determined by flow cytometry. All data were gated on CD11c⁺ cells. The change in mean fluorescence intensity (MFI) from PELC@PE to PELC@MN is indicated. The data are representative of three independent experiments. The results demonstrated that emulsified particles with monodisperse nanosized distribution could dramatically induce activation of BMDCs in vitro, compared with polydisperse ones.



Supplementary Figure S3. IHC staining of T-cell subsets in nasal mucosal tissues following intranasal vaccination with protein antigen adjuvanted with different formulations. The mice were intranasally vaccinated with OVA (100 μ g per dose) alone or adjuvanted with either PELC@PE or PELC@MN, once a week for 3 weeks. One week after the final vaccination, the nasal mucosal tissues (three mice per group) were prepared for IHC staining of T-cell subsets. The brown signals (arrows) indicate IHC-positive cells (magnification, 400x). Scale bars, 100 μ m. The results are representative of three independent experiments.

Supplementary Table S1. Complete list of microarray selected hits having a p-value ≤ 0.05 and a fold change $\geq |1.5|$. Data are expressed as the average fold change of three repeats in each treatment group (PELC@PE vs PBS)

Transcript ID	Gene Symbol	Gene Name	PELC@PE vs PBS	
			p-value	Fold-Change
17511643	Ces1a	carboxylesterase 1A [Mus musculus (house mouse)]	0.005	3.940
17482290	Acsm4	acyl-CoA synthetase medium-chain family member 4 [Mus musculus (house mouse)]	0.032	2.665
17481252	Olf635	olfactory receptor 635 [Mus musculus (house mouse)]	0.025	2.536
17229050	Fmo6	flavin containing monooxygenase 6 [Mus musculus (house mouse)]	0.040	2.506
17361878	Slc22a20	Mus musculus solute carrier family 22 (organic anion transporter), member 20 (Slc22a20), mRNA	0.049	2.498
17378035	Bpifb6	BPI fold containing family B, member 6 [Mus musculus (house mouse)]	0.029	2.402
17359918	Elovl3	elongation of very long chain fatty acids (FEN1/Elo2, SUR4/Elo3, yeast)-like 3 [Mus musculus (house mouse)]	0.024	2.350
17483975	5430419D17Rik	RIKEN cDNA 5430419D17 gene	0.038	2.294
17529227	unknown	Unknown	0.046	2.261
17536538	Awat1	acyl-CoA wax alcohol acyltransferase 1 [Mus musculus (house mouse)]	0.038	2.215
17333292	Slc22a2	solute carrier family 22 (organic cation transporter), member 2 [Mus musculus (house mouse)]	0.042	2.180
17378072	Bpifb4	BPI fold containing family B, member 4 [Mus musculus (house mouse)]	0.030	2.180
17387638	Olf1042	olfactory receptor 1042 [Mus musculus (house mouse)]	0.023	2.137
17513135	Ldhd	lactate dehydrogenase D [Mus musculus (house mouse)]	0.029	2.137
17494154	Olf578	olfactory receptor 578 [Mus musculus (house mouse)]	0.043	2.078
17423019	Sdr16c6	short chain dehydrogenase/reductase family 16C, member 6 [Mus musculus (house mouse)]	0.031	2.061
17326933	Krtap6-3	keratin associated protein 6-3 [Mus musculus (house mouse)]	0.012	2.057
17376191	Tgm3	transglutaminase 3, E polypeptide [Mus musculus (house mouse)]	0.005	2.049
17296080	unknown	Unknown	0.013	2.046

Transcript ID	Gene Symbol	Gene Name	PELC@PE vs PBS	
			p-value	Fold-Change
17503926	Mt4	metallothionein 4 [Mus musculus (house mouse)]	0.008	2.006
17387758	Olf1128	olfactory receptor 1128 [Mus musculus (house mouse)]	0.032	1.999
17429290	Olf1328	olfactory receptor 1328 [Mus musculus (house mouse)]	0.032	1.983
17387612	Olf1002	olfactory receptor 1002 [Mus musculus (house mouse)]	0.033	1.981
17416685	unknown	Unknown	0.009	1.979
17517360	Sln	sarcolipin [(house mouse)]	0.031	1.965
17448997	Nmu	neuromedin U [Mus musculus (house mouse)]	0.016	1.952
17494422	Olf655	olfactory receptor 655 [Mus musculus (house mouse)]	0.002	1.947
17481359	Olf689	olfactory receptor 689 [Mus musculus (house mouse)]	0.040	1.943
17352957	Dsc1	desmocollin 1 [(house mouse)]	0.027	1.938
17467519	Igkv8-30	immunoglobulin kappa chain variable 8-30 [Mus musculus]	0.023	1.933
17499613	Defb3	defensin beta 3 [(house mouse)]	0.041	1.910
17417924	unknown	Unknown	0.002	1.890
17537906	Kir3dl1	killer cell immunoglobulin-like receptor, three domains, long cytoplasmic tail, 1 [Mus musculus (house mouse)]	0.022	1.884
17343856	Btnl5	butyrophilin-like 5 [Mus musculus (house mouse)]	0.022	1.862
17525141	Gm1110	predicted gene 1110	0.000	1.847
17246435	Olf810	olfactory receptor 810 [Mus musculus (house mouse)]	0.023	1.819
17322026	Krt2	keratin 2 [(house mouse)]	0.037	1.819
17225253	Kcnj13	potassium inwardly-rectifying channel, subfamily J, member 13 [Mus musculus (house mouse)]	0.022	1.812
17494457	Olf675	olfactory receptor 675 [Mus musculus (house mouse)]	0.037	1.812
17429586	unknown	Unknown	0.038	1.801
17494170	Olf603	olfactory receptor 603 [Mus musculus (house mouse)]	0.041	1.797

Transcript ID	Gene Symbol	Gene Name	PELC@PE vs PBS	
			p-value	Fold-Change
17211347	Tfap2b	transcription factor AP-2 beta [Mus musculus (house mouse)]	0.029	1.795
17326887	ORF63	Map3k7 C-terminal like [Mus musculus (house mouse)]	0.027	1.786
17329207	2310042E22Rik	transmembrane epididymal family member 3 [Mus musculus (house mouse)]	0.008	1.778
17337618	Olf128	olfactory receptor 128 [Mus musculus (house mouse)]	0.006	1.773
17358825	I830012O16Rik	interferon-induced protein with tetratricopeptide repeats 3B [Mus musculus (house mouse)]	0.034	1.763
17337580	Olf111	olfactory receptor 111 [Mus musculus (house mouse)]	0.003	1.758
17507665	AF366264	cDNA sequence AF366264 [(house mouse)]	0.043	1.758
17516145	Olf1894	olfactory receptor 894 [Mus musculus (house mouse)]	0.027	1.756
17494267	Olf1640	olfactory receptor 640 [Mus musculus (house mouse)]	0.031	1.751
17494115	Olf1553	olfactory receptor 553 [Mus musculus (house mouse)]	0.004	1.747
17421168	unknown	Unknown	0.009	1.730
17421327	unknown	Unknown	0.022	1.727
17494144	Olf1569	olfactory receptor 569 [Mus musculus (house mouse)]	0.008	1.718
17494214	Olf168	olfactory receptor 68 [Mus musculus (house mouse)]	0.049	1.716
17212301	Tmem182	transmembrane protein 182 [(house mouse)]	0.016	1.706
17539494	Ace2	angiotensin I converting enzyme (peptidyl-dipeptidase A) 2 [Mus musculus (house mouse)]	0.002	1.697
17285631	Gpx6	glutathione peroxidase 6 [Mus musculus (house mouse)]	0.010	1.697
17265524	unknown	Unknown	0.048	1.696
17411101	unknown	Unknown	0.008	1.692
17516120	Olf145	olfactory receptor 145 [Mus musculus (house mouse)]	0.002	1.689
17481182	Olf1594	olfactory receptor 594 [Mus musculus (house mouse)]	0.002	1.681

Transcript ID	Gene Symbol	Gene Name	PELC@PE vs PBS	
			p-value	Fold-Change
17317428	Gsdmc	gasdermin C [(house mouse)]	0.018	1.680
17379992	Sall4	sal-like 4 (Drosophila) [(house mouse)]	0.046	1.676
17385028	unknown	Unknown	0.005	1.676
17529307	Elovl4	elongation of very long chain fatty acids (FEN1/Elo2, SUR4/Elo3, yeast)-like 4 [Mus musculus (house mouse)]	0.035	1.676
17318008	2300005B03Rik	secreted Ly6/Plaur domain containing 2 [Mus musculus (house mouse)]	0.038	1.673
17382592	Ptgds	prostaglandin D2 synthase (brain) [(house mouse)]	0.022	1.673
17544277	unknown	Unknown	0.003	1.672
17367644	Il1f8	interleukin 1 family, member 8 [(house mouse)]	0.035	1.671
17528214	unknown	Unknown	0.028	1.668
17226164	unknown	Unknown	0.011	1.668
17366922	Mir669m-1	microRNA 669m-1 [Mus musculus (house mouse)]	0.028	1.667
17494394	Trim30a	tripartite motif-containing 30A [(house mouse)]	0.002	1.662
17540378	Maob	monoamine oxidase B [(house mouse)]	0.049	1.654
17357416	unknown	Unknown	0.037	1.653
17449445	unknown	Unknown	0.012	1.653
17237975	unknown	Unknown	0.018	1.652
17407431	Lce1a1	late cornified envelope 1A1 [Mus musculus (house mouse)]	0.011	1.651
17499576	Defb34	defensin beta 34 [Mus musculus (house mouse)]	0.024	1.643
17404337	Cpa3	carboxypeptidase A3, mast cell [Mus musculus (house mouse)]	0.040	1.640
17525712	Olf937	olfactory receptor 937 [Mus musculus (house mouse)]	0.011	1.628
17274021	Osr1	odd-skipped related 1 (Drosophila) [Mus musculus (house mouse)]	0.002	1.621
17481155	Olf937	olfactory receptor 568 [Mus musculus (house mouse)]	0.031	1.621
17487054	Psg26	pregnancy-specific glycoprotein 26 [Mus musculus (house mouse)]	0.002	1.621
17366884	unknown	Unknown	0.030	1.620

Transcript ID	Gene Symbol	Gene Name	PELC@PE vs PBS	
			p-value	Fold-Change
17477266	Klk5	kallikrein related-peptidase 5 [(house mouse)]	0.026	1.616
17516143	Olf893	olfactory receptor 893 [Mus musculus (house mouse)]	0.017	1.614
17367666	Il1f5	interleukin 1 family, member 5 (delta) [(house mouse)]	0.028	1.614
17284654	unknown	Unknown	0.037	1.598
17399981	Rptn	repetin [(house mouse)]	0.034	1.592
17265818	Olf410	olfactory receptor 410 [Mus musculus (house mouse)]	0.041	1.592
17387810	Olf1166	olfactory receptor 1166 [Mus musculus (house mouse)]	0.037	1.592
17379887	unknown	Unknown	0.020	1.588
17407439	Lce1a2	late cornified envelope 1A2 [Mus musculus (house mouse)]	0.038	1.587
17372888	Olf1151	olfactory receptor 1151 [Mus musculus (house mouse)]	0.027	1.586
17333812	Vmn2r101	vomer nasal 2, receptor 101 [Mus musculus (house mouse)]	0.017	1.582
17367659	Il1f6	interleukin 1 family, member 6 [(house mouse)]	0.039	1.582
17277760	5430427M07Rik	RIKEN cDNA 5430427M07 gene [Mus musculus (house mouse)]	0.008	1.569
17304901	3425401B19Rik	RIKEN cDNA 3425401B19 gene [Mus musculus (house mouse)]	0.043	1.558
17257327	unknown	Unknown	0.016	1.554
17521068	unknown	Unknown	0.006	1.548
17265526	Nlrp1c	NLR family, pyrin domain containing 1C	0.004	1.546
17271143	Cacng1	calcium channel, voltage-dependent, gamma subunit 1 [Mus musculus (house mouse)]	0.035	1.543
17355076	unknown	Unknown	0.022	1.539
17322099	Krt78	keratin 78 [(house mouse)]	0.009	1.535
17370345	Olf348	olfactory receptor 348 [Mus musculus (house mouse)]	0.044	1.527
17257651	unknown	Unknown	0.037	1.519
17517105	Il18	interleukin 18 [(house mouse)]	0.010	1.515

Transcript ID	Gene Symbol	Gene Name	PELC@PE vs PBS	
			p-value	Fold-Change
17264946	Chrn1	cholinergic receptor, nicotinic, beta polypeptide 1 (muscle) [Mus musculus (house mouse)]	0.048	1.514
17512868	Chst4	carbohydrate (chondroitin 6/keratan) sulfotransferase 4 [Mus musculus (house mouse)]	0.021	1.513
17499723	LOC100505096	alpha-defensin 20-like mRNA [Mus musculus]	0.039	1.511
17482230	Acsm5	acyl-CoA synthetase medium-chain family member 5 [Mus musculus (house mouse)]	0.003	1.510
17349304	Tslp	thymic stromal lymphopoietin [(house mouse)]	0.029	1.510
17482310	Acsm3	acyl-CoA synthetase medium-chain family member 3 [Mus musculus (house mouse)]	0.039	1.508
17337614	Olf127	olfactory receptor 127 [Mus musculus (house mouse)]	0.002	1.506
17285240	unknown	Unknown	0.003	1.503
17291222	Hist2h3b	histone cluster 2, H3b [(house mouse)]	0.014	1.502
17372351	Neurod1	neurogenic differentiation 1 [(house mouse)]	0.009	-1.501
17377523	unknown	Unknown	0.010	-1.503
17411172	unknown	Unknown	0.026	-1.503
17303494	unknown	Unknown	0.028	-1.507
17404652	unknown	Unknown	0.000	-1.509
17444481	Bhlha15	basic helix-loop-helix family, member a15 [Mus musculus (house mouse)]	0.042	-1.509
17396339	unknown	Unknown	0.003	-1.510
17544740	Kir3dl2	killer cell immunoglobulin-like receptor, three domains, long cytoplasmic tail, 2 [Mus musculus (house mouse)]	0.037	-1.512
17510626	unknown	Unknown	0.009	-1.512
17330649	Gm17783	predicted gene, 17783 [Mus musculus]	0.027	-1.518
17483383	Snora30	small nucleolar RNA, H/ACA box 30	0.044	-1.520
17214899	Gm7609	predicted pseudogene 7609 [(house mouse)]	0.014	-1.522
17347983	unknown	Unknown	0.002	-1.525
17247375	unknown	Unknown	0.019	-1.532
17449372	Ugt2b38	UDP glucuronosyltransferase 2 family, polypeptide B38 [Mus musculus (house mouse)]	0.038	-1.539

Transcript ID	Gene Symbol	Gene Name	PELC@PE vs PBS	
			p-value	Fold-Change
17423802	unknown	Unknown	0.034	-1.541
17546790	unknown	Unknown	0.007	-1.544
17249034	unknown	Unknown	0.001	-1.545
17304848	unknown	Unknown	0.014	-1.555
17467427	unknown	Unknown	0.016	-1.555
17299119	unknown	Unknown	0.010	-1.562
17459095	unknown	Unknown	0.001	-1.562
17464713	unknown	Unknown	0.016	-1.566
17465339	unknown	Unknown	0.007	-1.571
17411905	unknown	Unknown	0.006	-1.576
17218042	unknown	Unknown	0.031	-1.582
17302354	unknown	Unknown	0.014	-1.585
17476637	unknown	Unknown	0.001	-1.588
17476671	unknown	Unknown	0.026	-1.597
17257593	unknown	Unknown	0.025	-1.597
17474128	unknown	Unknown	0.012	-1.604
17520288	unknown	Unknown	0.007	-1.605
17344750	H2-M9	histocompatibility 2, M region locus 9 [(house mouse)]	0.017	-1.611
17455210	Gm5565	predicted gene 5565 [Mus musculus]	0.001	-1.629
17225085	unknown	Unknown	0.047	-1.634
17374848	unknown	Unknown	0.000	-1.639
17268376	unknown	Unknown	0.034	-1.641
17232731	Rnu3a	U3A small nuclear RNA [Mus musculus]	0.025	-1.643
17219865	unknown	Unknown	0.033	-1.652
17486216	Vmn2r32	vomeronasal 2, receptor 32 [Mus musculus]	0.044	-1.654
17402979	unknown	Unknown	0.015	-1.660
17324398	Snora81	small nucleolar RNA, H/ACA box 81	0.033	-1.670
17448146	unknown	Unknown	0.025	-1.672

Transcript ID	Gene Symbol	Gene Name	PELC@PE vs PBS	
			p-value	Fold-Change
17529690	unknown	Unknown	0.041	-1.676
17476877	unknown	Unknown	0.007	-1.682
17504002	unknown	Unknown	0.042	-1.691
17234423	Derl3	Der1-like domain family, member 3 [(house mouse)]	0.044	-1.694
17430885	unknown	Unknown	0.012	-1.697
17325721	unknown	Unknown	0.008	-1.698
17312079	unknown	Unknown	0.044	-1.699
17308827	unknown	Unknown	0.037	-1.700
17274408	Gm17758	predicted gene, 17758 [Mus musculus (house mouse)]	0.017	-1.701
17513974	unknown	Unknown	0.005	-1.704
17411133	unknown	Unknown	0.010	-1.706
17526803	unknown	Unknown	0.006	-1.725
17398719	unknown	Unknown	0.031	-1.727
17441622	unknown	Unknown	0.035	-1.730
17491851	unknown	Unknown	0.011	-1.744
17340397	Nanp	N-acetylneuraminic acid phosphatase [Mus musculus (house mouse)]	0.041	-1.755
17536036	unknown	Unknown	0.023	-1.770
17339172	unknown	Unknown	0.008	-1.784
17513854	unknown	Unknown	0.001	-1.786
17244862	unknown	Unknown	0.013	-1.788
17229574	unknown	Unknown	0.023	-1.792
17458950	Vmn1r13	vomeronasal 1 receptor 13 [Mus musculus (house mouse)]	0.002	-1.798
17385838	unknown	Unknown	0.001	-1.809
17463617	unknown	Unknown	0.008	-1.816
17512852	unknown	Unknown	0.017	-1.825
17477184	Klk14	kallikrein related-peptidase 14 [(house mouse)]	0.003	-1.827
17514343	unknown	Unknown	0.049	-1.834

Transcript ID	Gene Symbol	Gene Name	PELC@PE vs PBS	
			p-value	Fold-Change
17494221	Hbb-b1	hemoglobin, beta adult major chain [(house mouse)]	0.022	-1.852
17248973	Olf1387	olfactory receptor 1387 [Mus musculus (house mouse)]	0.041	-1.877
17486261	Vmn2r41	Vmn2r4vomeronasal 2, receptor 41 [(house mouse)]1	0.038	-1.889
17249513	unknown	Unknown	0.033	-1.891
17248494	unknown	Unknown	0.001	-1.894
17508566	unknown	Unknown	0.021	-2.043
17536044	Gm5938	predicted gene 5938 [Mus musculus (house mouse)]	0.016	-2.292
17514349	unknown	Unknown	0.038	-2.468
17540497	unknown	Unknown	0.022	-3.332

Supplementary Table S2. Complete list of microarray selected hits having a p-value ≤ 0.05 and a fold change $\geq |1.5|$. Data are expressed as the average fold change of three repeats in each treatment group (PELC@MN vs PBS)

Transcript ID	Gene Symbol	Gene Name	PELC@MN vs PBS	
			p-value	Fold-Change
17481252	Olf635	olfactory receptor 635 [Mus musculus (house mouse)]	0.023	2.600
17398018	unknown	Unknown	0.003	2.558
17501516	unknown	Unknown	0.027	2.451
17395969	unknown	Unknown	0.032	2.399
17511643	Ces1a	carboxylesterase 1A [Mus musculus (house mouse)]	0.025	2.392
17238667	Olf787	olfactory receptor 787 [Mus musculus (house mouse)]	0.020	2.375
17459306	unknown	Unknown	0.003	2.322
17238661	Olf782	olfactory receptor 782 [Mus musculus (house mouse)]	0.020	2.234
17476604	Abpe	secretoglobin, family 2B, member 2 [Mus musculus (house mouse)]	0.012	2.204
17372781	Olf1029	olfactory receptor 1029 [Mus musculus (house mouse)]	0.037	2.193
17459294	Igkv1-133	immunoglobulin kappa variable 1-133 [Mus musculus (house mouse)]	0.027	2.187
17525712	Olf937	olfactory receptor 937 [Mus musculus (house mouse)]	0.002	2.184
17467379	unknown	Unknown	0.001	2.146
17278328	Serpina3n	serine (or cysteine) peptidase inhibitor, clade A, member 3N [Mus musculus (house mouse)]	0.027	2.143
17471788	LOC100048471	Unknown	0.007	2.141
17544277	unknown	Unknown	0.001	2.129
17225982	unknown	Unknown	0.023	2.094
17306130	unknown	Unknown	0.025	2.090
17507665	AF366264	cDNA sequence AF366264 [(house mouse)]	0.019	2.079
17288302	Rsl1	regulator of sex limited protein 1 [(house mouse)]	0.003	2.034
17535269	1700020N15Rik	1700020N15Rik RIKEN cDNA 1700020N15 gene [(house mouse)]	0.005	1.974
17494422	Olf655	olfactory receptor 655 [Mus musculus (house mouse)]	0.002	1.968

Transcript ID	Gene Symbol	Gene Name	PELC@MN vs PBS	
			p-value	Fold-Change
]		
17494144	Olf569	olfactory receptor 569 [Mus musculus (house mouse)]	0.004	1.955
17481194	Olf598	olfactory receptor 598 [Mus musculus (house mouse)]	0.025	1.952
17284654	unknown	Unknown	0.012	1.947
17378072	Bpifb4	BPI fold containing family B, member 4 [Mus musculus (house mouse)]	0.049	1.944
17387758	Olf1128	olfactory receptor 1128 [Mus musculus (house mouse)]	0.043	1.876
17214892	unknown	Unknown	0.025	1.871
17467534	Igkv6-23	immunoglobulin kappa variable 6-23 [(house mouse)]	0.019	1.864
17547178	unknown	Unknown	0.006	1.847
17516120	Olf145	olfactory receptor 145 [Mus musculus (house mouse)]	0.001	1.837
17237975	unknown	Unknown	0.010	1.810
17542098	unknown	Unknown	0.035	1.804
17494447	Olf668	olfactory receptor 668 [Mus musculus (house mouse)]	0.049	1.796
17481141	Olf557	olfactory receptor 557 [Mus musculus (house mouse)]	0.014	1.787
17499723	LOC100505096	alpha-defensin 20-like mRNA [Mus musculus]	0.013	1.779
17226164	unknown	Unknown	0.008	1.758
17387810	Olf1166	olfactory receptor 1166 [Mus musculus (house mouse)]	0.020	1.757
17348400	Gata6	GATA binding protein 6 [(house mouse)]	0.030	1.755
17425200	unknown	Unknown	0.021	1.744
17337601	unknown	Unknown	0.036	1.740
17494256	Olf64	olfactory receptor 640 [Mus musculus (house mouse)]	0.047	1.728
17546995	unknown	Unknown	0.021	1.721
17372742	unknown	Unknown	0.002	1.720
17457295	unknown	Unknown	0.023	1.709

Transcript ID	Gene Symbol	Gene Name	PELC@MN vs PBS	
			p-value	Fold-Change
17300024	unknown	Unknown	0.018	1.704
17232176	Taar2	trace amine-associated receptor 2 [(house mouse)]	0.046	1.704
17543742	unknown	Unknown	0.022	1.701
17494319	OlfR649	olfactory receptor 649 [Mus musculus (house mouse)]	0.002	1.697
17285842	Hist2h3b	histone cluster 2, H3b [(house mouse)]	0.015	1.691
17238689	OlfR808	olfactory receptor 808 [Mus musculus (house mouse)]	0.005	1.688
17320811	unknown	Unknown	0.014	1.684
17290195	LOC639910	mouse hypothetical protein LOC639910	0.023	1.684
17304271	unknown	Unknown	0.017	1.682
17486646	Vmn1r86	vomer nasal 1 receptor 62 [(house mouse)]	0.006	1.677
17234363	4933407G14Rik	RIKEN cDNA 4933407G14 gene [(house mouse)]	0.014	1.675
17543139	Mageb1	melanoma antigen, family B, 1 [(house mouse)]	0.011	1.669
17474692	unknown	Unknown	0.037	1.669
17257327	unknown	Unknown	0.010	1.660
17464037	unknown	Unknown	0.042	1.654
17335983	Gm9705	cytochrome P450, family 4, subfamily f, polypeptide 37	0.026	1.654
17435170	6030443J06Rik	RIKEN cDNA 6030443J06 gene [(house mouse)]	0.003	1.653
17467516	Igk-V28	immunoglobulin kappa chain variable 28 (V28) [(house mouse)]	0.012	1.650
17284484	Ighg	immunoglobulin heavy chain complex [(house mouse)]	0.003	1.649
17494394	Trim30a	tripartite motif-containing 30A [(house mouse)]	0.002	1.646
17444059	unknown	Unknown	0.000	1.643
17533454	unknown	Unknown	0.009	1.641
17326933	Krtap6-3	keratin associated protein 6-3 [Mus musculus (house mouse)]	0.040	1.640
17516143	OlfR893	olfactory receptor 893 [Mus musculus (house mouse)]	0.015	1.637
17299158	LOC100044625	Unknown	0.037	1.635

Transcript ID	Gene Symbol	Gene Name	PELC@MN vs PBS	
			p-value	Fold-Change
17311733	Fer1l6	fer-1-like 6 (C. elegans) [(house mouse)]	0.002	1.631
17494267	Olf640	olfactory receptor 640 [Mus musculus (house mouse)]	0.047	1.630
17389132	Gm13939	pluripotency associated transcript 8 [Mus musculus (house mouse)]	0.021	1.629
17257597	unknown	Unknown	0.043	1.627
17503926	Mt4	metallothionein 4 [(house mouse)]	0.027	1.622
17364365	unknown	Unknown	0.043	1.622
17246435	Olf810	olfactory receptor 810 [Mus musculus (house mouse)]	0.044	1.618
17417819	Olf1339	olfactory receptor 1339 [Mus musculus (house mouse)]	0.008	1.617
17379887	unknown	Unknown	0.018	1.616
17385369	unknown	Unknown	0.015	1.615
17513963	unknown	Unknown	0.034	1.614
17337614	Olf127	olfactory receptor 127 [Mus musculus (house mouse)]	0.001	1.607
17516274	Olf961	olfactory receptor 961 [Mus musculus (house mouse)]	0.000	1.607
17305937	Olf726	olfactory receptor 726 [Mus musculus (house mouse)]	0.028	1.606
17299965	unknown	Unknown	0.020	1.603
17298729	unknown	Unknown	0.012	1.603
17495622	Gp2	glycoprotein 2 (zymogen granule membrane) [(house mouse)]	0.018	1.602
17512891	LOC100861869	Unknown	0.017	1.601
17233792	unknown	Unknown	0.007	1.599
17372771	Olf1022	olfactory receptor 1022 [Mus musculus (house mouse)]	0.021	1.595
17481334	Dub1	ubiquitin specific peptidase 17-like A [(house mouse)]	0.015	1.592
17294034	Zfp71-rs1	zinc finger protein 71, related sequence 1 [Mus musculus]	0.021	1.590
17482230	Acs5	acyl-CoA synthetase medium-chain family member 5 [Mus musculus (house mouse)]	0.002	1.587

Transcript ID	Gene Symbol	Gene Name	PELC@MN vs PBS	
			p-value	Fold-Change
17262218	Gm12185	predicted gene 12185 [(house mouse)]	0.022	1.585
17536653	unknown	Unknown	0.022	1.577
17474278	Ceacam5	carcinoembryonic antigen-related cell adhesion molecule 5 [Mus musculus (house mouse)]	0.017	1.576
17501308	Gm2921	predicted gene 2921 [(house mouse)]	0.040	1.569
17355076	unknown	Unknown	0.019	1.569
17291222	Hist2h3b	histone cluster 2, H3b [(house mouse)]	0.010	1.568
17502366	Olf372	olfactory receptor 372 [Mus musculus (house mouse)]	0.023	1.566
17239769	Taar9	trace amine-associated receptor 9 [(house mouse)]	0.040	1.564
17516147	Olf143	olfactory receptor 143 [Mus musculus (house mouse)]	0.024	1.558
17459005	Vmn1r28	vomerolnasal 1 receptor 28 [Mus musculus (house mouse)]	0.022	1.554
17287792	unknown	Unknown	0.045	1.549
17308759	4930444M15Rik	RIKEN cDNA 4930444M15 gene [(house mouse)]	0.025	1.548
17506945	unknown	Unknown	0.035	1.547
17448226	unknown	Unknown	0.029	1.546
17481182	Olf594	olfactory receptor 594 [Mus musculus (house mouse)]	0.004	1.545
17211562	unknown	Unknown	0.043	1.545
17228291	unknown	Unknown	0.021	1.544
17544162	unknown	Unknown	0.021	1.544
17366922	Mir669m-1	microRNA 669m-1 [(house mouse)]	0.045	1.543
17319753	unknown	Unknown	0.010	1.542
17512868	Chst4	carbohydrate (chondroitin 6/keratan) sulfotransferase 4 [Mus musculus (house mouse)]	0.018	1.542
17421327	unknown	Unknown	0.045	1.541
17481215	Olf617	olfactory receptor 617 [Mus musculus (house mouse)]	0.034	1.539
17381626	8030442B05Rik	RIKEN cDNA 8030442B05 gene [Mus musculus (house mouse)]	0.001	1.537

Transcript ID	Gene Symbol	Gene Name	PELC@MN vs PBS	
			p-value	Fold-Change
17471744	Klra14	killer cell lectin-like receptor subfamily A, member 14, pseudogene [Mus musculus (house mouse)]	0.015	1.536
17277659	BB287469	expressed sequence BB287469 [(house mouse)]	0.023	1.536
17412636	unknown	Unknown	0.027	1.535
17411101	unknown	Unknown	0.016	1.533
17374188	Olf1285	olfactory receptor 1285 [Mus musculus (house mouse)]	0.031	1.532
17467477	unknown	Unknown	0.018	1.531
17311310	unknown	Unknown	0.046	1.530
17531799	Mir128-2	microRNA 128-2 [(house mouse)]	0.014	1.529
17378238	1700007I08Rik	actin-like 10 [Mus musculus (house mouse)]	0.008	1.527
17280932	unknown	Unknown	0.047	1.526
17494115	Olf553	olfactory receptor 553 [Mus musculus (house mouse)]	0.010	1.524
17543889	unknown	Unknown	0.008	1.524
17284423	Ighg	immunoglobulin heavy chain complex [(house mouse)]	0.047	1.522
17489954	LOC546957	Unknown	0.032	1.518
17241729	Phyhip1	phytanoyl-CoA hydroxylase interacting protein-like [Mus musculus (house mouse)]	0.002	1.516
17481196	Olf599	olfactory receptor 599 [Mus musculus (house mouse)]	0.041	1.512
17278713	Rtl1	retrotransposon-like 1 [(house mouse)]	0.002	1.511
17513641	Slc7a5	solute carrier family 7 (cationic amino acid transporter, y+ system), member 5 [Mus musculus (house mouse)]	0.002	1.509
17481171	Olf584	olfactory receptor 584 [Mus musculus (house mouse)]	0.048	1.507
17421103	B330016D10Rik	RIKEN cDNA B330016D10 gene [Mus musculus (house mouse)]	0.021	1.507
17546158	unknown	Unknown	0.024	1.507
17331436	unknown	Unknown	0.048	1.505
17514355	unknown	Unknown	0.022	1.503

Transcript ID	Gene Symbol	Gene Name	PELC@MN vs PBS	
			p-value	Fold-Change
17525710	Olf936	olfactory receptor 936 [Mus musculus (house mouse)]	0.024	1.502
17478799	unknown	Unknown	0.004	1.502
17503808	unknown	Unknown	0.010	1.501
17299135	unknown	Unknown	0.009	1.501
17285240	unknown	Unknown	0.003	1.500
17423802	unknown	Unknown	0.040	-1.503
17278236	unknown	Unknown	0.027	-1.504
17324125	Polr2h	polymerase (RNA) II (DNA directed) polypeptide H [Mus musculus (house mouse)]	0.047	-1.505
17432521	C87977	expressed sequence C87977 [(house mouse)]	0.047	-1.507
17324475	A230028O05Rik	RIKEN cDNA A230028O05 gene [Mus musculus (house mouse)]	0.021	-1.508
17337152	H2-Q10	H2-Q10 histocompatibility 2, Q region locus 10 [(house mouse)]	0.013	-1.509
17363755	unknown	Unknown	0.046	-1.510
17344126	Hspa1b	heat shock protein 1B [(house mouse)]	0.039	-1.510
17476637	unknown	Unknown	0.001	-1.512
17404652	unknown	Unknown	0.000	-1.515
17425028	Hemgn	hemogen	0.043	-1.518
17325365	unknown	Unknown	0.002	-1.521
17402979	unknown	Unknown	0.027	-1.522
17482912	unknown	Unknown	0.002	-1.524
17408123	Cd160	CD160 antigen [Mus musculus (house mouse)]	0.036	-1.527
17240085	unknown	Unknown	0.035	-1.527
17235855	unknown	Unknown	0.009	-1.528
17317264	unknown	Unknown	0.026	-1.531
17490953	unknown	Unknown	0.001	-1.535
17439365	unknown	Unknown	0.015	-1.539
17474361	Sycp1-ps1	synaptonemal complex protein 1, pseudogene 1 [Mus musculus (house mouse)]	0.043	-1.542

Transcript ID	Gene Symbol	Gene Name	PELC@MN vs PBS	
			p-value	Fold-Change
17439764	unknown	Unknown	0.032	-1.548
17396339	unknown	Unknown	0.003	-1.548
17380093	unknown	Unknown	0.025	-1.555
17476877	unknown	Unknown	0.013	-1.558
17280254	Gm5433	predicted gene 5433 [(house mouse)]	0.047	-1.558
17519314	unknown	Unknown	0.025	-1.560
17302354	unknown	Unknown	0.016	-1.561
17325721	unknown	Unknown	0.014	-1.564
17307963	Ebf2	early B cell factor 2 [(house mouse)]	0.014	-1.568
17430209	unknown	Unknown	0.002	-1.568
17266182	unknown	Unknown	0.018	-1.572
17218760	unknown	Unknown	0.015	-1.572
17268376	unknown	Unknown	0.043	-1.577
17219865	unknown	Unknown	0.043	-1.578
17513974	unknown	Unknown	0.009	-1.589
17232731	Rnu3a	U3A small nuclear RNA [(house mouse)]	0.031	-1.595
17455210	Gm5565	predicted gene 5565 [Mus musculus (house mouse)]	0.002	-1.596
17518318	unknown	Unknown	0.013	-1.599
17293982	Zfp874b	zinc finger protein 874b [Mus musculus (house mouse)]	0.021	-1.604
17300030	unknown	Unknown	0.024	-1.606
17512852	unknown	Unknown	0.034	-1.620
17381190	Gm14496	predicted gene 14496 [(house mouse)]	0.027	-1.620
17438993	unknown	Unknown	0.009	-1.625
17512084	unknown	Unknown	0.021	-1.630
17398719	unknown	Unknown	0.043	-1.631
17244862	unknown	Unknown	0.023	-1.633
17494431	Dub3	ubiquitin specific peptidase 17-like E [Mus musculus (house mouse)]	0.035	-1.641

Transcript ID	Gene Symbol	Gene Name	PELC@MN vs PBS	
			p-value	Fold-Change
17347983	unknown	Unknown	0.001	-1.647
17366810	Mir669a-1	microRNA 669a-1 [(house mouse)]	0.010	-1.673
17366846	Mir669a-1	microRNA 669a-1 [(house mouse)]	0.010	-1.673
17339172	unknown	Unknown	0.010	-1.697
17409619	unknown	Unknown	0.032	-1.703
17331824	Cldn17	claudin 17 [(house mouse)]	0.048	-1.704
17404230	Gm5150	predicted gene 5150 [(house mouse)]	0.015	-1.709
17520288	unknown	Unknown	0.004	-1.712
17406323	MNE1	meiotic nuclear divisions 1 [(house mouse)]	0.013	-1.726
17526803	unknown	Unknown	0.006	-1.742
17393535	unknown	Unknown	0.025	-1.743
17225113	Gm19524	predicted gene 19524 [(house mouse)]	0.006	-1.756
17285527	unknown	Unknown	0.006	-1.761
17289009	Hapln1	hyaluronan and proteoglycan link protein 1 [Mus musculus (house mouse)]	0.043	-1.761
17395039	unknown	Unknown	0.047	-1.787
17296565	Gm2888	predicted gene 2888 [(house mouse)]	0.025	-1.797
17400118	unknown	Unknown	0.025	-1.802
17225085	unknown	Unknown	0.026	-1.815
17324398	Snora81	small nucleolar RNA, H/ACA box 81 [Mus musculus (house mouse)]	0.020	-1.818
17218042	unknown	Unknown	0.013	-1.820
17477184	Klk14	kallikrein related-peptidase 14 [Mus musculus (house mouse)]	0.003	-1.827
17429918	unknown	Unknown	0.001	-1.849
17529690	unknown	Unknown	0.024	-1.851
17464713	unknown	Unknown	0.005	-1.856
17312079	unknown	Unknown	0.026	-1.883
17430885	unknown	Unknown	0.005	-1.928
17385838	unknown	Unknown	0.000	-1.938

Transcript ID	Gene Symbol	Gene Name	PELC@MN vs PBS	
			p-value	Fold-Change
17292327	Mirlet7f-1	microRNA let7f-1 [(house mouse)]	0.019	-1.949
17528615	unknown	Unknown	0.036	-1.968
17248494	unknown	Unknown	0.001	-2.061
17270607	unknown	Unknown	0.002	-2.080
17249513	unknown	Unknown	0.020	-2.117
17491851	unknown	Unknown	0.004	-2.132
17494221	Hbb-b1	hemoglobin, beta adult major chain [(house mouse)]	0.011	-2.155
17248973	Olf1387	olfactory receptor 1387 [Mus musculus (house mouse)]	0.022	-2.173
17505877	Clec3a	C-type lectin domain family 3, member a [(house mouse)]	0.027	-2.389
17540497	unknown	Unknown	0.031	-2.961

Supplementary Table S3. Complete list of microarray selected hits having a p-value ≤ 0.05 and a fold change $\geq |1.5|$. Data are expressed as the average fold change of three repeats in each treatment group (PELC@MN vs PELC@PE)

Transcript ID	Gene Symbol	Gene Name	PELC@MN vs PELC@PE	
			p-value	Fold-Change
17322507	Dnase1	deoxyribonuclease I [(house mouse)]	0.021	5.442
17399858	Sprr2a2	small proline-rich protein 2A2 [(house mouse)]	0.032	2.661
17472129	Gucy2c	guanylate cyclase 2c [(house mouse)]	0.023	2.629
17368200	Gm13539	predicted gene 13539 [(house mouse)]	0.014	2.432
17476604	Abpe	secretoglobin, family 2B, member 2 [Mus musculus (house mouse)]	0.009	2.357
17234423	Derl3	Der1-like domain family, member 3 [(house mouse)]	0.010	2.285
17495622	Gp2	glycoprotein 2 (zymogen granule membrane) [(house mouse)]	0.003	2.243
17459398	unknown	Unknown	0.040	2.191
17300040	unknown	Unknown	0.034	2.181
17214892	unknown	Unknown	0.012	2.171
17274188	unknown	Unknown	0.012	2.156
17305381	unknown	Unknown	0.040	2.144
17444481	Bhlha15	basic helix-loop-helix family, member a15 [Mus musculus (house mouse)]	0.006	2.089
17308827	unknown	Unknown	0.016	1.992
17337679	Gm17495	exocrine gland secreted peptide 8 [Mus musculus (house mouse)]	0.020	1.984
17514328	unknown	Unknown	0.013	1.981
17467534	Igkv6-23	immunoglobulin kappa variable 6-23 [(house mouse)]	0.015	1.943
17295569	Naip2	NLR family, apoptosis inhibitory protein 2 [(house mouse)]	0.025	1.922
17514355	unknown	Unknown	0.005	1.907
17427928	Dio1	deiodinase, iodothyronine, type I [(house mouse)]	0.039	1.900
17329316	Dgkg	diacylglycerol kinase, gamma [(house mouse)]	0.024	1.871
17459306	unknown	Unknown	0.008	1.868
17374848	unknown	Unknown	0.000	1.863
17325044	Slc12a8	solute carrier family 12 (potassium/chloride	0.015	1.859

Transcript ID	Gene Symbol	Gene Name	PELC@MN vs PELC@PE	
			p-value	Fold-Change
		transporters), member 8 [Mus musculus (house mouse)]		
17514346	unknown	Unknown	0.023	1.854
17300024	unknown	Unknown	0.011	1.846
17234363	4933407G14Rik	RIKEN cDNA 4933407G14 gene [Mus musculus (house mouse)]	0.008	1.843
17284585	V165-D-J-C mu	IgM variable region [Mus musculus (house mouse)]	0.041	1.835
17476671	unknown	Unknown	0.011	1.828
17340397	Nanp	N-acetylneuraminic acid phosphatase [Mus musculus (house mouse)]	0.035	1.805
17467447	unknown	Unknown	0.040	1.802
17504002	unknown	Unknown	0.032	1.779
17299119	unknown	Unknown	0.004	1.771
17273240	Pycr1	pyrroline-5-carboxylate reductase 1 [Mus musculus (house mouse)]	0.008	1.763
17457737	Try10	trypsin 10 [(house mouse)]	0.028	1.760
17387886	Olf1218	olfactory receptor 1218 [Mus musculus (house mouse)]	0.007	1.758
17536036	unknown	Unknown	0.024	1.755
17467379	unknown	Unknown	0.003	1.751
17493395	unknown	Unknown	0.038	1.743
17536052	Obp1b	odorant binding protein 1B [Mus musculus (house mouse)]	0.022	1.741
17216127	Gm7889	predicted gene 7889 [Mus musculus (house mouse)]	0.048	1.736
17341303	Fpr-rs6	formyl peptide receptor, related sequence 6 [Mus musculus (house mouse)]	0.036	1.730
17238652	unknown	Unknown	0.034	1.717
17220186	unknown	Unknown	0.046	1.716
17398018	unknown	Unknown	0.019	1.715
17373634	unknown	Unknown	0.037	1.709
17289016	Gm4117	predicted gene 4117 [Mus musculus (house mouse)]	0.015	1.702
17540743	Slx	Sycp3 like X-linked [Mus musculus (house mouse)]	0.042	1.690

Transcript ID	Gene Symbol	Gene Name	PELC@MN vs PELC@PE	
			p-value	Fold-Change
17274405	Gm19924	predicted gene 19924 [Mus musculus (house mouse)]	0.009	1.688
17333776	Vmn2r96	vomeronasal 2, receptor 96 [Mus musculus (house mouse)]	0.009	1.687
17520111	unknown	Unknown	0.014	1.686
17544870	Ripply1	rippy transcriptional repressor 1 [Mus musculus (house mouse)]	0.017	1.684
17219164	Sh2d1b2	SH2 domain containing 1B2 [(house mouse)]	0.030	1.674
17546382	unknown	Unknown	0.013	1.673
17458950	Vmn1r13	vomeronasal 1 receptor 13 [(house mouse)]	0.004	1.669
17424968	Gm12409	predicted gene 12409 [Mus musculus (house mouse)]	0.000	1.668
17471744	Klra14	killer cell lectin-like receptor subfamily A, member 14, pseudogene [Mus musculus (house mouse)]	0.009	1.661
17217237	Gm10538	predicted gene 10538 [Mus musculus (house mouse)]	0.047	1.659
17463451	unknown	Unknown	0.022	1.655
17341905	Rab26	RAB26, member RAS oncogene family [Mus musculus (house mouse)]	0.048	1.631
17543139	Mageb1	melanoma antigen, family B, 1 [(house mouse)]	0.013	1.629
17284390	unknown	Unknown	0.003	1.629
17458377	Gimap1	GTPase, IMAP family member 1 [Mus musculus (house mouse)]	0.008	1.622
17543742	unknown	Unknown	0.030	1.620
17299158	LOC100044625	Unknown	0.039	1.617
17238671	Olf790	olfactory receptor 790 [Mus musculus (house mouse)]	0.004	1.598
17284423	Ighg	immunoglobulin heavy chain complex [(house mouse)]	0.034	1.592
17306991	Gzmd	granzyme D [(house mouse)]	0.002	1.592
17388347	unknown	Unknown	0.006	1.587
17388681	Rag2	recombination activating gene 2 [Mus musculus (house mouse)]	0.027	1.581
17315178	Nr4a1	nuclear receptor subfamily 4, group A, member 1 [Mus musculus (house mouse)]	0.006	1.580
17294051	unknown	Unknown	0.003	1.578
17472023	Mansc1	MANSC domain containing 1 [Mus musculus (house	0.021	1.572

Transcript ID	Gene Symbol	Gene Name	PELC@MN vs PELC@PE	
			p-value	Fold-Change
		mouse)]		
17366864	unknown	Unknown	0.026	1.571
17325933	Gm6030	predicted gene 6030 [Mus musculus (house mouse)]	0.018	1.571
17535108	unknown	Unknown	0.009	1.571
17480489	unknown	Unknown	0.009	1.569
17448146	unknown	Unknown	0.038	1.568
17459423	Igkv4-53	immunoglobulin kappa variable 4-53 [Mus musculus (house mouse)]	0.037	1.564
17445992	unknown	Unknown	0.029	1.556
17344696	unknown	Unknown	0.013	1.551
17493310	unknown	Unknown	0.048	1.549
17486646	Vmn1r86	vomer nasal 1 receptor 86 [(house mouse)]	0.011	1.545
17502603	Rasd2	RASD family, member 2 [(house mouse)]	0.017	1.543
17448595	Gabra4	gamma-aminobutyric acid (GABA) A receptor, subunit alpha 4 [Mus musculus (house mouse)]	0.049	1.541
17342770	Spdef	SAM pointed domain containing ets transcription factor [Mus musculus (house mouse)]	0.004	1.537
17424822	Gne	glucosamine (UDP-N-acetyl)-2-epimerase/N-acetylmannosamine kinase [Mus musculus (house mouse)]	0.029	1.536
17233507	BB019430	expressed sequence BB019430 [Mus musculus (house mouse)]	0.001	1.535
17237280	Phlda1	pleckstrin homology like domain, family A, member 1 [Mus musculus (house mouse)]	0.025	1.535
17328742	Slc7a4	solute carrier family 7 (cationic amino acid transporter, y+ system), member 4 [Mus musculus (house mouse)]	0.005	1.535
17244911	unknown	Unknown	0.013	1.533
17387723	Olf1099	olfactory receptor 1099 [Mus musculus (house mouse)]	0.022	1.533
17524336	Olf850	olfactory receptor 850 [Mus musculus (house mouse)]	0.024	1.531
17535269	1700020N15Rik	1700020N15Rik RIKEN cDNA 1700020N15 gene [(house mouse)]	0.026	1.531
17279948	unknown	Unknown	0.005	1.528
17444059	unknown	Unknown	0.000	1.523

Transcript ID	Gene Symbol	Gene Name	PELC@MN vs PELC@PE	
			p-value	Fold-Change
17523201	Myrip	myosin VIIA and Rab interacting protein [Mus musculus (house mouse)]	0.006	1.519
17284512	unknown	Unknown	0.046	1.519
17298729	unknown	Unknown	0.018	1.518
17314679	Tuba1b	tubulin, alpha 1B [Mus musculus (house mouse)]	0.009	1.518
17413942	unknown	Unknown	0.029	1.516
17489962	unknown	Unknown	0.049	1.514
17536736	Gjb1	gap junction protein, beta 1 [(house mouse)]	0.007	1.514
17546995	unknown	Unknown	0.048	1.512
17491505	unknown	Unknown	0.004	1.512
17284484	Ighg	immunoglobulin heavy chain complex [(house mouse)]	0.005	1.512
17535045	Gm14718	predicted gene 14718 [Mus musculus (house mouse)]	0.005	1.509
17467365	unknown	Unknown	0.000	1.502
17424848	unknown	Unknown	0.024	1.502
17450501	Gbp10	guanylate-binding protein 10 [(house mouse)]	0.047	-2.017
17464943	Ppp1r3a	protein phosphatase 1, regulatory (inhibitor) subunit 3A [Mus musculus (house mouse)]	0.014	-2.024
17345797	Apobec2	apolipoprotein B mRNA editing enzyme, catalytic polypeptide 2 [Mus musculus (house mouse)]	0.035	-2.026
17371296	Xirp2	xin actin-binding repeat containing 2 [Mus musculus (house mouse)]	0.032	-2.078
17292327	Mirlet7f-1	microRNA let7f-1 [(house mouse)]	0.013	-2.098
17232453	Trdn	triadin [Mus musculus (house mouse)]	0.014	-2.183
17467519	Igkv8-30	immunoglobulin kappa chain variable 8-30 [Mus musculus]	0.012	-2.226
17416685	unknown	Unknown	0.002	-2.681

Supplementary Table S4. Core response gene list

Transcript ID	Gene Symbol	Gene Name
Mucosal/cell permeability		
17361878	Slc22a20	Mus musculus solute carrier family 22 (organic anion transporter), member 20 (Slc22a20), mRNA
17378035	Bpifb6	BPI fold containing family B, member 6 [Mus musculus (house mouse)]
17378072	Bpifb4	BPI fold containing family B, member 4 [Mus musculus (house mouse)]
17517360	Sln	sarcolipin [(house mouse)]
17352957	Dsc1	desmocollin 1 [(house mouse)]
17225253	Kcnj13	potassium inwardly-rectifying channel, subfamily J, member 13 [Mus musculus (house mouse)]
17271143	Cacng1	calcium channel, voltage-dependent, gamma subunit 1 [Mus musculus (house mouse)]
17495622	Gp2	glycoprotein 2 (zymogen granule membrane) [(house mouse)]
17513641	Slc7a5	solute carrier family 7 (cationic amino acid transporter, y+ system), member 5 [Mus musculus (house mouse)]
17331824	Cldn17	claudin 17 [(house mouse)]
17325044	Slc12a8	solute carrier family 12 (potassium/chloride transporters), member 8 [Mus musculus (house mouse)]
17328742	Slc7a4	solute carrier family 7 (cationic amino acid transporter, y+ system), member 4 [Mus musculus (house mouse)]
17536736	Gjb1	gap junction protein, beta 1 [(house mouse)]
Immune responses		
17467519	Igkv8-30	immunoglobulin kappa chain variable 8-30 [Mus musculus]
17499613	Defb3	defensin beta 3 [(house mouse)]
17537906	Kir3dl1	killer cell immunoglobulin-like receptor, three domains, long cytoplasmic tail, 1 [Mus musculus (house mouse)]
17343856	Btnl5	butyrophilin-like 5 [Mus musculus (house mouse)]
17326887	ORF63	Map3k7 C-terminal like [Mus musculus (house mouse)]
17358825	I830012O16Rik	interferon-induced protein with tetratricopeptide repeats 3B [Mus musculus (house mouse)]
17367644	Il1f8	interleukin 1 family, member 8 [(house mouse)]
17494394	Trim30a	tripartite motif-containing 30A [(house mouse)]
17499576	Defb34	defensin beta 34 [Mus musculus (house mouse)]
17404337	Cpa3	carboxypeptidase A3, mast cell [Mus musculus (house mouse)]

Transcript ID	Gene Symbol	Gene Name
17487054	Psg26	pregnancy-specific glycoprotein 26 [Mus musculus (house mouse)]
17367666	Il1f5	interleukin 1 family, member 5 (delta) [(house mouse)]
17367659	Il1f6	interleukin 1 family, member 6 [(house mouse)]
17517105	Il18	interleukin 18 [(house mouse)]
17512868	Chst4	carbohydrate (chondroitin 6/keratan) sulfotransferase 4 [Mus musculus (house mouse)]
17499723	LOC100505096	alpha-defensin 20-like mRNA [Mus musculus]
17349304	Tslp	thymic stromal lymphopoietin [(house mouse)]
17544740	Kir3dl2	killer cell immunoglobulin-like receptor, three domains, long cytoplasmic tail, 2 [Mus musculus (house mouse)]
17344750	H2-M9	histocompatibility 2, M region locus 9 [(house mouse)]
17459294	Igkv1-133	immunoglobulin kappa variable 1-133 [Mus musculus (house mouse)]
17467534	Igkv6-23	immunoglobulin kappa variable 6-23 [(house mouse)]
17348400	Gata6	GATA binding protein 6 [(house mouse)]
17467516	Igk-V28	immunoglobulin kappa chain variable 28 (V28) [(house mouse)]
17284423	Ighg	immunoglobulin heavy chain complex [(house mouse)]
17284484	Ighg	immunoglobulin heavy chain complex [(house mouse)]
17481334	Dub1	ubiquitin specific peptidase 17-like A [(house mouse)]
17471744	Klra14	killer cell lectin-like receptor subfamily A, member 14, pseudogene [Mus musculus (house mouse)]
17337152	H2-Q10	H2-Q10 histocompatibility 2, Q region locus 10 [(house mouse)]
17344126	Hspa1b	heat shock protein 1B [(house mouse)]
17408123	Cd160	CD160 antigen [Mus musculus (house mouse)]
17307963	Ebf2	early B cell factor 2 [(house mouse)]
17404230	Gm5150	predicted gene 5150 [(house mouse)]
17472129	Gucy2c	guanylate cyclase 2c [(house mouse)]
17284585	V165-D-J-C mu	IgM variable region [Mus musculus (house mouse)]
17341303	Fpr-rs6	formyl peptide receptor, related sequence 6 [Mus musculus (house mouse)]
17219164	Sh2d1b2	SH2 domain containing 1B2 [(house mouse)]
17458377	Gimap1	GTPase, IMAP family member 1 [Mus musculus (house mouse)]
17306991	Gzmd	granzyme D [(house mouse)]

Transcript ID	Gene Symbol	Gene Name
17388681	Rag2	recombination activating gene 2 [Mus musculus (house mouse)]
17315178	Nr4a1	nuclear receptor subfamily 4, group A, member 1 [Mus musculus (house mouse)]
17459423	Igkv4-53	immunoglobulin kappa variable 4-53 [Mus musculus (house mouse)]
17342770	Spdef	SAM pointed domain containing ets transcription factor [Mus musculus (house mouse)]
17450501	Gbp10	guanylate-binding protein 10 [(house mouse)]
Fatty acid metabolism		
17482290	Acsm4	acyl-CoA synthetase medium-chain family member 4 [Mus musculus (house mouse)]
17359918	Elovl3	elongation of very long chain fatty acids (FEN1/Elo2, SUR4/Elo3, yeast)-like 3 [Mus musculus (house mouse)]
17536538	Awat1	acyl-CoA wax alcohol acyltransferase 1 [Mus musculus (house mouse)]
17333292	Slc22a2	solute carrier family 22 (organic cation transporter), member 2 [Mus musculus (house mouse)]
17529307	Elovl4	elongation of very long chain fatty acids (FEN1/Elo2, SUR4/Elo3, yeast)-like 4 [Mus musculus (house mouse)]
17482230	Acsm5	acyl-CoA synthetase medium-chain family member 5 [Mus musculus (house mouse)]
17482310	Acsm3	acyl-CoA synthetase medium-chain family member 3 [Mus musculus (house mouse)]
Tumor-associated		
17317428	Gsdmc	gasdermin C [(house mouse)]
17318008	2300005B03Rik	secreted Ly6/Plaur domain containing 2 [Mus musculus (house mouse)]
17543139	Mageb1	melanoma antigen, family B, 1 [(house mouse)]
17345797	Apobec2	apolipoprotein B mRNA editing enzyme, catalytic polypeptide 2 [Mus musculus (house mouse)]
17477184	Klk14	kallikrein related-peptidase 14 [(house mouse)]
Neurotransduction		
17481252	Olfr635	olfactory receptor 635 [Mus musculus (house mouse)]
17387638	Olfr1042	olfactory receptor 1042 [Mus musculus (house mouse)]
17494154	Olfr578	olfactory receptor 578 [Mus musculus (house mouse)]
17387758	Olfr1128	olfactory receptor 1128 [Mus musculus (house mouse)]
17429290	Olfr1328	olfactory receptor 1328 [Mus musculus (house mouse)]

Transcript ID	Gene Symbol	Gene Name
17387612	Olfr1002	olfactory receptor 1002 [Mus musculus (house mouse)]
17448997	Nmu	neuromedin U [Mus musculus (house mouse)]
17494422	Olfr655	olfactory receptor 655 [Mus musculus (house mouse)]
17481359	Olfr689	olfactory receptor 689 [Mus musculus (house mouse)]
17246435	Olfr810	olfactory receptor 810 [Mus musculus (house mouse)]
17494457	Olfr675	olfactory receptor 675 [Mus musculus (house mouse)]
17494170	Olfr603	olfactory receptor 603 [Mus musculus (house mouse)]
17337618	Olfr128	olfactory receptor 128 [Mus musculus (house mouse)]
17337580	Olfr111	olfactory receptor 111 [Mus musculus (house mouse)]
17516145	Olfr894	olfactory receptor 894 [Mus musculus (house mouse)]
17494267	Olfr640	olfactory receptor 640 [Mus musculus (house mouse)]
17494115	Olfr553	olfactory receptor 553 [Mus musculus (house mouse)]
17494144	Olfr569	olfactory receptor 569 [Mus musculus (house mouse)]
17494214	Olfr68	olfactory receptor 68 [Mus musculus (house mouse)]
17516120	Olfr145	olfactory receptor 145 [Mus musculus (house mouse)]
17481182	Olfr594	olfactory receptor 594 [Mus musculus (house mouse)]
17540378	Maob	monoamine oxidase B [(house mouse)]
17525712	Olfr937	olfactory receptor 937 [Mus musculus (house mouse)]
17481155	Olfr568	olfactory receptor 568 [Mus musculus (house mouse)]
17516143	Olfr893	olfactory receptor 893 [Mus musculus (house mouse)]
17265818	Olfr410	olfactory receptor 410 [Mus musculus (house mouse)]
17387810	Olfr1166	olfactory receptor 1166 [Mus musculus (house mouse)]
17372888	Olfr1151	olfactory receptor 1151 [Mus musculus (house mouse)]
17333812	Vmn2r101	vomer nasal 2, receptor 101 [Mus musculus (house mouse)]
17370345	Olfr348	olfactory receptor 348 [Mus musculus (house mouse)]
17264946	Chrn1	cholinergic receptor, nicotinic, beta polypeptide 1 (muscle) [Mus musculus (house mouse)]
17337614	Olfr127	olfactory receptor 127 [Mus musculus (house mouse)]
17372351	Neurod1	neurogenic differentiation 1 [(house mouse)]
17486216	Vmn2r32	vomer nasal 2, receptor 32 [Mus musculus]

Transcript ID	Gene Symbol	Gene Name
17274408	Gm17758	predicted gene, 17758 [Mus musculus (house mouse)]
17458950	Vmn1r13	vomeronasal 1 receptor 13 [Mus musculus (house mouse)]
17248973	Olfr1387	olfactory receptor 1387 [Mus musculus (house mouse)]
17486261	Vmn2r41	Vmn2r4vomeronasal 2, receptor 41 [(house mouse)]1
17238667	Olfr787	olfactory receptor 787 [Mus musculus (house mouse)]
17238661	Olfr782	olfactory receptor 782 [Mus musculus (house mouse)]
17372781	Olfr1029	olfactory receptor 1029 [Mus musculus (house mouse)]
17481194	Olfr598	olfactory receptor 598 [Mus musculus (house mouse)]
17516120	Olfr145	olfactory receptor 145 [Mus musculus (house mouse)]
17494447	Olfr668	olfactory receptor 668 [Mus musculus (house mouse)]
17481141	Olfr557	olfactory receptor 557 [Mus musculus (house mouse)]
17387810	Olfr1166	olfactory receptor 1166 [Mus musculus (house mouse)]
17494319	Olfr649	olfactory receptor 649 [Mus musculus (house mouse)]
17238689	Olfr808	olfactory receptor 808 [Mus musculus (house mouse)]
17486646	Vmn1r86	vomeronasal 1 receptor 62 [(house mouse)]
17417819	Olfr1339	olfactory receptor 1339 [Mus musculus (house mouse)]
17516274	Olfr961	olfactory receptor 961 [Mus musculus (house mouse)]
17305937	Olfr726	olfactory receptor 726 [Mus musculus (house mouse)]
17372771	Olfr1022	olfactory receptor 1022 [Mus musculus (house mouse)]
17502366	Olfr372	olfactory receptor 372 [Mus musculus (house mouse)]
17516147	Olfr143	olfactory receptor 143 [Mus musculus (house mouse)]
17459005	Vmn1r28	vomeronasal 1 receptor 28 [Mus musculus (house mouse)]
17481215	Olfr617	olfactory receptor 617 [Mus musculus (house mouse)]
17531799	Mir128-2	microRNA 128-2 [(house mouse)]
17481196	Olfr599	olfactory receptor 599 [Mus musculus (house mouse)]
17481171	Olfr584	olfactory receptor 584 [Mus musculus (house mouse)]
17525710	Olfr936	olfactory receptor 936 [Mus musculus (house mouse)]
17248973	Olfr1387	olfactory receptor 1387 [Mus musculus (house mouse)]
17368200	Gm13539	predicted gene 13539 [(house mouse)]

Transcript ID	Gene Symbol	Gene Name
17387886	Olfr1218	olfactory receptor 1218 [Mus musculus (house mouse)]
17333776	Vmn2r96	vomeronasal 2, receptor 96 [Mus musculus (house mouse)]
17458950	Vmn1r13	vomeronasal 1 receptor 13 [(house mouse)]
17238671	Olfr790	olfactory receptor 790 [Mus musculus (house mouse)]
17387723	Olfr1099	olfactory receptor 1099 [Mus musculus (house mouse)]
17524336	Olfr850	olfactory receptor 850 [Mus musculus (house mouse)]
oxidation and reduction		
17285631	Gpx6	glutathione peroxidase 6 [Mus musculus (house mouse)]
17273240	Pycr1	pyrroline-5-carboxylate reductase 1 [Mus musculus (house mouse)]
Cell death		
17513135	Ldhd	lactate dehydrogenase D [Mus musculus (house mouse)]
17265526	Nlrp1c	NLR family, pyrin domain containing 1C
17494431	Dub3	ubiquitin specific peptidase 17-like E [Mus musculus (house mouse)]
17292327	Mirlet7f-1	microRNA let7f-1 [(house mouse)]
17322507	Dnase1	deoxyribonuclease I [(house mouse)]
17295569	Naip2	NLR family, apoptosis inhibitory protein 2 [(house mouse)]
17237280	Phlda1	pleckstrin homology like domain, family A, member 1 [Mus musculus (house mouse)]
Xenobiotic excretion		
17229050	Fmo6	flavin containing monooxygenase 6 [Mus musculus (house mouse)]
Others		
17423019	Sdr16c6	short chain dehydrogenase/reductase family 16C, member 6 [Mus musculus (house mouse)]
17326933	Krtap6-3	keratin associated protein 6-3 [Mus musculus (house mouse)]
17376191	Tgm3	transglutaminase 3, E polypeptide [Mus musculus (house mouse)]
17322026	Krt2	keratin 2 [(house mouse)]
17211347	Tfap2b	transcription factor AP-2 beta [Mus musculus (house mouse)]
17329207	2310042E22Rik	transmembrane epididymal family member 3 [Mus musculus (house mouse)]
17507665	AF366264	cDNA sequence AF366264 [(house mouse)]
17212301	Tmem182	transmembrane protein 182 [(house mouse)]

Transcript ID	Gene Symbol	Gene Name
17539494	Ace2	angiotensin I converting enzyme (peptidyl-dipeptidase A) 2 [Mus musculus (house mouse)]
17379992	Sall4	sal-like 4 (Drosophila) [(house mouse)]
17382592	Ptgds	prostaglandin D2 synthase (brain) [(house mouse)]
17366922	Mir669m-1	microRNA 669m-1 [Mus musculus (house mouse)]
17407431	Lce1a1	late cornified envelope 1A1 [Mus musculus (house mouse)]
17274021	Osr1	odd-skipped related 1 (Drosophila) [Mus musculus (house mouse)]
17477266	Klk5	kallikrein related-peptidase 5 [(house mouse)]
17399981	Rptn	repetin [(house mouse)]
17407439	Lce1a2	late cornified envelope 1A2 [Mus musculus (house mouse)]
17277760	5430427M07Rik	RIKEN cDNA 5430427M07 gene [Mus musculus (house mouse)]
17304901	3425401B19Rik	RIKEN cDNA 3425401B19 gene [Mus musculus (house mouse)]
17322099	Krt78	keratin 78 [(house mouse)]
17291222	Hist2h3b	histone cluster 2, H3b [(house mouse)]
17444481	Bhlha15	basic helix-loop-helix family, member a15 [Mus musculus (house mouse)]
17330649	Gm17783	predicted gene, 17783 [Mus musculus]
17483383	Snora30	small nucleolar RNA, H/ACA box 30
17214899	Gm7609	predicted pseudogene 7609 [(house mouse)]
17449372	Ugt2b38	UDP glucuronosyltransferase 2 family, polypeptide B38 [Mus musculus (house mouse)]
17455210	Gm5565	predicted gene 5565 [Mus musculus]
17232731	Rnu3a	U3A small nuclear RNA [Mus musculus]
17324398	Snora81	small nucleolar RNA, H/ACA box 81
17234423	Der13	Der1-like domain family, member 3 [(house mouse)]
17340397	Nanp	N-acetylneuraminic acid phosphatase [Mus musculus (house mouse)]
17494221	Hbb-b1	hemoglobin, beta adult major chain [(house mouse)]
17536044	Gm5938	predicted gene 5938 [Mus musculus (house mouse)]
17476604	Abpe	secretoglobin, family 2B, member 2 [Mus musculus (house mouse)]
17278328	Serpina3n	serine (or cysteine) peptidase inhibitor, clade A, member 3N [Mus musculus (house mouse)]
17507665	AF366264	cDNA sequence AF366264 [(house mouse)]

Transcript ID	Gene Symbol	Gene Name
17288302	Rsl1	regulator of sex limited protein 1 [(house mouse)]
17535269	1700020N15Rik	1700020N15Rik RIKEN cDNA 1700020N15 gene [(house mouse)]
17232176	Taar2	trace amine-associated receptor 2 [(house mouse)]
17290195	LOC639910	mouse hypothetical protein LOC639910
17234363	4933407G14Rik	RIKEN cDNA 4933407G14 gene [(house mouse)]
17435170	6030443J06Rik	RIKEN cDNA 6030443J06 gene [(house mouse)]
17389132	Gm13939	pluripotency associated transcript 8 [Mus musculus (house mouse)]
17503926	Mt4	metallothionein 4 [(house mouse)]
17294034	Zfp71-rs1	zinc finger protein 71, related sequence 1 [Mus musculus]
17474278	Ceacam5	carcinoembryonic antigen-related cell adhesion molecule 5 [Mus musculus (house mouse)]
17239769	Taar9	trace amine-associated receptor 9 [(house mouse)]
17308759	4930444M15Rik	RIKEN cDNA 4930444M15 gene [(house mouse)]
17381626	8030442B05Rik	RIKEN cDNA 8030442B05 gene [Mus musculus (house mouse)]
17277659	BB287469	expressed sequence BB287469 [(house mouse)]
17378238	1700007I08Rik	actin-like 10 [Mus musculus (house mouse)]
17241729	Phyhipl	phytanoyl-CoA hydroxylase interacting protein-like [Mus musculus (house mouse)]
17278713	Rtl1	retrotransposon-like 1 [(house mouse)]
17421103	B330016D10Rik	RIKEN cDNA B330016D10 gene [Mus musculus (house mouse)]
17324125	Polr2h	polymerase (RNA) II (DNA directed) polypeptide H [Mus musculus (house mouse)]
17432521	C87977	expressed sequence C87977 [(house mouse)]
17324475	A230028O05Rik	RIKEN cDNA A230028O05 gene [Mus musculus (house mouse)]
17474361	Sycp1-ps1	synaptonemal complex protein 1, pseudogene 1 [Mus musculus (house mouse)]
17280254	Gm5433	predicted gene 5433 [(house mouse)]
17293982	Zfp874b	zinc finger protein 874b [Mus musculus (house mouse)]
17381190	Gm14496	predicted gene 14496 [(house mouse)]
17366810	Mir669a-1	microRNA 669a-1 [(house mouse)]
17366846	Mir669a-1	microRNA 669a-1 [(house mouse)]

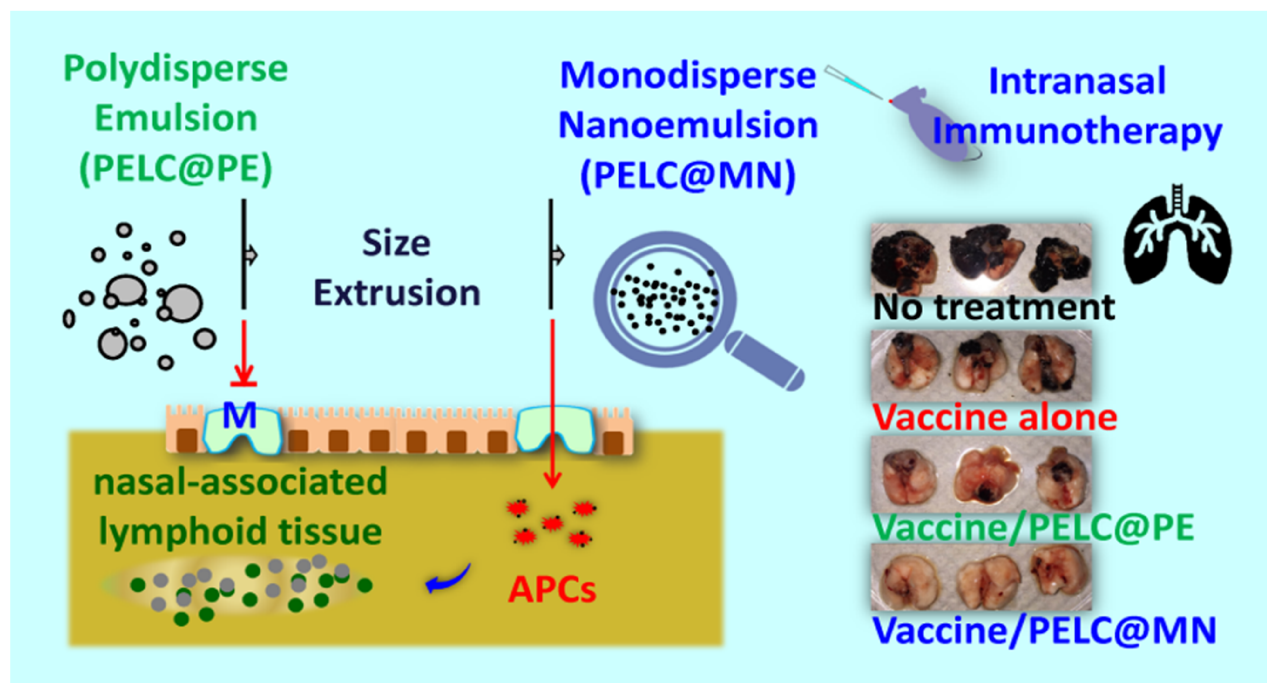
Transcript ID	Gene Symbol	Gene Name
17406323	MNE1	meiotic nuclear divisions 1 [(house mouse)]
17225113	Gm19524	predicted gene 19524 [(house mouse)]
17289009	Hapln1	hyaluronan and proteoglycan link protein 1 [Mus musculus (house mouse)]
17296565	Gm2888	predicted gene 2888 [(house mouse)]
17494221	Hbb-b1	hemoglobin, beta adult major chain [(house mouse)]
17505877	Clec3a	C-type lectin domain family 3, member a [(house mouse)]
17399858	Sprr2a2	small proline-rich protein 2A2 [(house mouse)]
17337679	Gm17495	exocrine gland secreted peptide 8 [Mus musculus (house mouse)]
17427928	Dio1	deiodinase, iodothyronine, type I [(house mouse)]
17329316	Dgkg	diacylglycerol kinase, gamma [(house mouse)]
17234363	4933407G14Rik	RIKEN cDNA 4933407G14 gene [Mus musculus (house mouse)]
17340397	Nanp	N-acetylneuraminic acid phosphatase [Mus musculus (house mouse)]
17457737	Try10	trypsin 10 [(house mouse)]
17536052	Obp1b	odorant binding protein 1B [Mus musculus (house mouse)]
17216127	Gm7889	predicted gene 7889 [Mus musculus (house mouse)]
17289016	Gm4117	predicted gene 4117 [Mus musculus (house mouse)]
17540743	Slx	Sycp3 like X-linked [Mus musculus (house mouse)]
17274405	Gm19924	predicted gene 19924 [Mus musculus (house mouse)]
17544870	Ripply1	rippy transcriptional repressor 1 [Mus musculus (house mouse)]
17424968	Gm12409	predicted gene 12409 [Mus musculus (house mouse)]
17217237	Gm10538	predicted gene 10538 [Mus musculus (house mouse)]
17341905	Rab26	RAB26, member RAS oncogene family [Mus musculus (house mouse)]
17472023	Mansc1	MANSC domain containing 1 [Mus musculus (house mouse)]
17325933	Gm6030	predicted gene 6030 [Mus musculus (house mouse)]
17502603	Rasd2	RASD family, member 2 [(house mouse)]
17448595	Gabra4	gamma-aminobutyric acid (GABA) A receptor, subunit alpha 4 [Mus musculus (house mouse)]
17424822	Gne	glucosamine (UDP-N-acetyl)-2-epimerase/N-acetylmannosamine kinase [Mus musculus (house mouse)]
17233507	BB019430	expressed sequence BB019430 [Mus musculus (house mouse)]

Transcript ID	Gene Symbol	Gene Name
17523201	Myrip	myosin VIIA and Rab interacting protein [<i>Mus musculus</i> (house mouse)]
17314679	Tuba1b	tubulin, alpha 1B [<i>Mus musculus</i> (house mouse)]
17535045	Gm14718	predicted gene 14718 [<i>Mus musculus</i> (house mouse)]
17464943	Ppp1r3a	protein phosphatase 1, regulatory (inhibitor) subunit 3A [<i>Mus musculus</i> (house mouse)]
17371296	Xirp2	xin actin-binding repeat containing 2 [<i>Mus musculus</i> (house mouse)]
17232453	Trdn	triadin [<i>Mus musculus</i> (house mouse)]

Graphical Abstract

Nanoemulsion adjuvantation strategy of tumor-associated antigen therapy rephrases mucosal and immunotherapeutic signatures following intranasal vaccination

Chung-Hsiung Huang, Chiung-Yi Huang, Hui-Min Ho, Ching-Hung Lee, Pang-Ti Lai, Suh-Chin Wu, Shih-Jen Liu, Ming-Hsi Huang



Nanoemulsion adjuvantation can facilitate the transportation of antigen across mucosal membrane to the nasal-associated lymphoid tissue, thereby rephrasing the immunotherapeutic signatures and improving the efficacy of tumor-associated antigen therapy against in situ and metastatic tumors.